Acta Mech 226, 745–768 (2015)
DOI 10.1007/s00707-014-1216-z

I. P. Pegios · S. Papargyri-Beskou · D. E. Beskos

Finite element static and stability analysis of gradient elastic beam structures

Received: 30 December 2013 / Revised: 23 April 2014 / Published online: 24 August 2014

Abstract In this paper, the static and stability stiffness matrices of a gradient elastic flexural Bernoulli–Euler beam finite element are analytically constructed with the aid of the basic and governing equations of equilibrium for that element. The flexural element has one node at every end with three degrees of freedom per node, i.e., the displacement, the slope and the curvature. The stability stiffness matrix incorporates the effect of axial compressive force on bending. Use of these stiffness matrices for a plane system of beams enables one through a finite element analysis to determine its response to static loading and its buckling load. Because the exact solution of the governing equation of the problem is used as the displacement function, the resulting stiffness matrices and the obtained structural responses are also exact. Examples are presented to illustrate the method and demonstrate its merits.

1 Introduction

Linear elastic bars, beams, plates and shells used in nanomechanical and nanoelectronic devices have extremely small dimensions, which are comparable to their microstructural internal lengths, and thus, their response to static or dynamic loads depends on their material microstructure (Senturia [1]). When these microstructural effects are important and since classical theory of elasticity is incapable of taking them into account, resort should be made to generalized or higher-order elasticity theories, which due to their nonlocal character and the inclusion of internal length parameters can adequately model them in a macroscopic manner. Among those theories, Mindlin's [2] general theory of elasticity with microstructure in its various forms and simplifications has found many applications in structural analysis of microstructures. In particular, the form II theory of Mindlin [2] associated with the second gradient of strain and consisting of just one constant (internal length) for the static case in addition to the other two classical elastic moduli, usually mentioned as the gradient theory of elasticity, has been extensively used during the last 15 years or so. Comprehensive literature reviews on the gradient elasticity theory and its applications in the solution of static and dynamic problems by analytical and numerical methods are those of Exadaktylos and Vardoulakis [3], Askes and Aifantis [4] and Tsinopoulos et al. [5].

Among the plethora of works on the subject of gradient elasticity as applied to static and dynamic problems, one can mention a few as representative cases of dealing with manifestations of microstructural effects modeled by gradient elasticity. Microstructural effects appear in the form of increased stiffness [6], size effects [7],

I. P. Pegios · S. Papargyri-Beskou
Department of Civil Engineering, Aristotle University of Thessaloniki, 54124 Thessaloníki, Greece

D. E. Beskos (✉)
Department of Civil Engineering, University of Patras, 26500 Patras, Greece
E-mail: d.e.beskos@upatras.gr

elimination of singularities [8], increase of buckling loads and natural frequencies [9] and wave dispersion [10].

For the particular case of the static and dynamic analysis of flexural gradient elastic beams, the structures considered in this paper, one can mention the works of Papargyri-Beskou et al. [11,12], Lam et al. [13], Giannakopoulos and Stamoulis [14], Kong et al. [15] and Papargyri-Beskou and Beskos [6] on gradient elastic Bernoulli–Euler beams and Papargyri-Beskou et al. [10], Wang et al. [16], Akgoz and Civalek [17] and Triantafyllou and Giannakopoulos [18] on gradient elastic Timoshenko beams. In all these works, the analysis was done by analytic methods and the beams were simple, statically determinate and under simple type of loading.

However, for statically indeterminate beams with complex type of loading and/or variable cross-section and especially for structures composed of beams, such as frames or gridworks, analytic methods become complicated, inefficient and hence impractical. For all the above cases, resort should be made to numerical methods of solution, such as the finite element method (FEM) [19]. Triantafyllou and Giannakopoulos [18], recognizing the problem, tried to provide analysis aids for simple gradient elastic statically determinate and indeterminate Timoshenko beams but they did not develop any numerical method of solution. It is really surprising that as reported in [5], various finite element and boundary element methods have been developed for the much more involved two- and three-dimensional gradient elastic solids and structures up to this year and none for beam structures consisting of very simple one-dimensional members. Artan and Batra [20] and Artan and Toksoz [21] employed the method of initial values (also known as the matrix transfer method) to determine the eigenfrequencies and buckling loads, respectively, of simple gradient elastic Bernoulli–Euler beams under various boundary conditions at their two ends. Their method is able to treat more complicated cases than purely analytical methods, e.g., indeterminate beams or beams composed of more than one member but is very complicated and lacks the generality, versatility and efficiency of the FEM, and for this reason, even though an old method, its use is very limited.

In this work, the static and stability stiffness matrices of a gradient elastic flexural Bernoulli–Euler beam finite element are analytically constructed with the aid of the basic and governing equations of equilibrium of that element and its associated possible boundary conditions as described in Papargyri-Beskou et al. [11]. Use of these stiffness matrices for a plane system of beams enables one through a finite element analysis to determine its response to static loading and its buckling load. Because the exact solution of the governing equation of the problem is used as the displacement function, the resulting stiffness matrices and the obtained structural response are also exact. Asiminas and Koumousis [22] have very recently constructed stiffness matrices for finite element analysis of gradient elastic Bernoulli–Euler plane beam structures on the basis of the theory in [11]. However, their displacement function is the usual cubic polynomial solution of the classical beam bending problem and as a result of that the resulting matrices are approximate. This implies that every physical member of the structure has to be discretized into a number of 2–3 finite elements for acceptable accuracy solutions. In contrast, because the stiffness matrices of the present work are exact, one can assign only one finite element per physical member and still obtain the exact solution. Of course, the expressions of the stiffness coefficients here are more complicated than those in [22] but they are in closed form, and hence, the additional computational effort is small.

Seven examples are presented to illustrate the method and demonstrate its merits. Five examples deal with static analysis of statically determinate and indeterminate beams of uniform and nonuniform cross-section and two examples with the determination of the buckling load of a beam under different types of nonclassical boundary conditions.

2 Gradient elastic beam theory

The basic and governing equations of a gradient elastic Bernoulli–Euler beam in bending under static lateral loading as well as the associated classical and nonclassical boundary conditions derived in Papargyri-Beskou et al. [11] are reproduced in this section for reasons of completeness and easy reference.

Consider a straight prismatic beam under a static lateral load $q(x)$ distributed along the longitudinal axis of the beam, as shown in Fig. 1. Thus, the loading plane is x–y, and the cross-section A of the beam is characterized by the two axes y and z with the former one being its axis of symmetry. Under the lateral load $q(x)$, the beam experiences bending in the x–y plane measured by its lateral deflection $v(x)$ along the x axis. Axial deformation of the beam is considered to be negligible. Assuming gradient elastic material behavior,

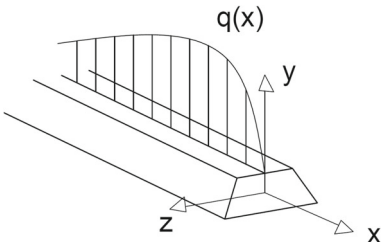

Fig. 1 Geometry and loading of a prismatic beam in bending

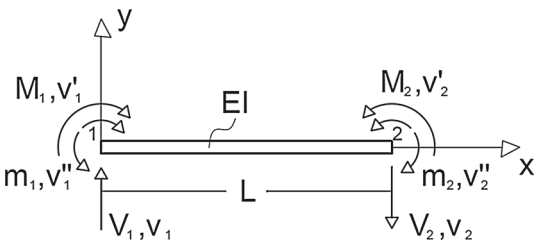

Fig. 2 Mechanics convention for generalized nodal forces and displacements of a gradient elastic flexural beam element

one has that the normal to the cross-section bending stress σ_x has the form

$$\sigma_x = E\left(\varepsilon_x - g^2\frac{\mathrm{d}^2\varepsilon_x}{\mathrm{d}x^2}\right), \tag{1}$$

where E is the modulus of elasticity, g is the gradient coefficient with dimensions of length (internal length representing the microstructural effects macroscopically) and ε_{x} is the normal bending strain expressed as

$$\varepsilon_x = -y\frac{\mathrm{d}^2 v}{\mathrm{d}x^2}. \tag{2}$$

Utilizing the kinematics of the Bernoulli–Euler theory, the constitutive relation (1) and the equilibrium of axial forces and bending moments, one can finally obtain the governing equations of equilibrium for the gradient elastic beam in terms of the lateral deflection $v(x)$ as [11]

$$\mathrm{EI}\left(\frac{\mathrm{d}^4 v}{\mathrm{d}x^4} - g^2\frac{\mathrm{d}^6 v}{\mathrm{d}x^6}\right) = -q(x), \tag{3}$$

where I is the cross-sectional moment of inertia about the z axis. The above equation, which is of the sixth degree, reduces to the classical one of the fourth degree for $g = 0$.

If one considers a beam element of length L with its two ends defined by $x = 0$ and $x = L$, as shown in Fig. 2, and makes use of a variational statement, he can recover the governing equation (3) and all possible classical and nonclassical boundary conditions so as to satisfy the following equations [11]:

$$\begin{gathered}
\left[V(L) - \mathrm{EI}[v'''(L) - g^2 v^{\mathrm{v}}(L)]\right]\delta v(L) - \left[V(0) - \mathrm{EI}[v'''(0) - g^2 v^{\mathrm{v}}(0)]\right]\delta v(0) = 0,\\
\left[M(L) - \mathrm{EI}[v''(L) - g^2 v^{\mathrm{IV}}(L)]\right]\delta v'(L) - \left[M(0) - \mathrm{EI}[v''(0) - g^2 v^{\mathrm{IV}}(0)]\right]\delta v'(0) = 0,\\
\left[m(L) - \mathrm{EI}g^2 v'''(L)\right]\delta v''(L) - \left[m(0) - \mathrm{EI}g^2 v'''(0)\right]\delta v''(0) = 0.
\end{gathered} \tag{4}$$

In the above, primes denote derivatives with respect to x, V is the shear force, M is the bending moment and m is the double bending moment due to the microstructure. This double moment m consists of two self-equilibrating moment vectors that do not contribute to the equilibrium equations but to the strain energy, as depicted in Fig. 2, where the positive directions of all forces and moments are also shown. It is observed that for $g = 0$, Eq. (4) reduces to the corresponding ones for the classical case. The term classical boundary conditions for the first two of Eqs. (4), used in this work and in most works of the pertinent literature, may not be correct in the sense that these two equations contain not only classical but also nonclassical terms as well. However, for

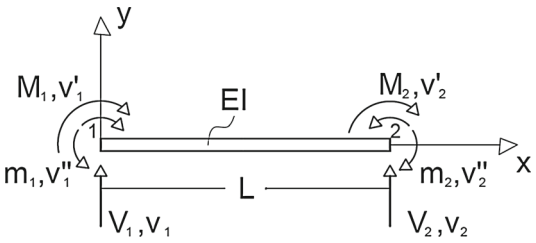

Fig. 3 Matrix convention for generalized nodal forces and displacements of a gradient elastic flexural beam element

$g = 0$, these equations reduce to the classical ones, while the third of Eqs. (4), consisting of only nonclassical terms, disappears.

If one assumes the four classical boundary conditions to be $v(0)$, $v(L)$, $v'(0)$ and $v'(L)$ prescribed and the nonclassical ones to be $v''(0)$ and $v''(L)$ prescribed, then $\delta v(0) = \delta v(L) = 0$, $\delta v'(0) = \delta v'(L) = 0$, $\delta v''(0) = \delta v''(L) = 0$ and Eq. (4) are all satisfied. In view of Eq. (4), one can observe that, when dealing with the classical boundary conditions, either the deflections v or the shear forces $V = \mathrm{EI}(v''' - g^2 v^{\mathrm{V}})$ and the strains (slopes) v' or the bending moments $M = \mathrm{EI}(v'' - g^2 v^{\mathrm{IV}})$ at the boundary of the beam have to be specified. For the case of the nonclassical boundary conditions, one has to specify either the boundary strain gradients (curvatures) v'' or the boundary double moments $m = \mathrm{EI}g^2 v'''$.

Consider now the previous beam of Figs. 1 and 2 without the lateral load $q(x)$ subjected to an axial compressive constant load P, which can cause flexural buckling for a certain value P_{cr} called the critical load or buckling load to be determined.

The governing equation of a beam in buckling as well as all possible boundary conditions can be obtained with the aid of a variational statement as described in detail in [11]. Thus, the governing equation of a beam in buckling is of the form

$$\mathrm{EI}\left(v^{\mathrm{IV}} - g^2 v^{\mathrm{VI}}\right) + P v'' = 0, \tag{5}$$

while the boundary conditions satisfy the equations

$$\begin{gathered}\left[V(L) - \left[P v'(L) + \mathrm{EI}\left[v'''(L) - g^2 v^{\mathrm{V}}(L)\right]\right]\right]\delta v(L) - \left[V(0) - \left[P v'(0) + \mathrm{EI}\left[v'''(0) - g^2 v^{\mathrm{V}}(0)\right]\right]\right]\delta v(0) = 0,\\ \left[M(L) - \mathrm{EI}[v''(L) - g^2 v^{\mathrm{IV}}(L)]\right]\delta v'(L) - \left[M(0) - \mathrm{EI}[v''(0) - g^2 v^{\mathrm{IV}}(0)]\right]\delta v'(0) = 0,\\ \left[m(L) - \mathrm{EI}g^2 v'''(L)\right]\delta v''(L) - \left[m(0) - \mathrm{EI}g^2 v'''(0)\right]\delta v''(0) = 0.\end{gathered} \tag{6}$$

It is easy to see that if g = 0 in Eqs. (5) and (6), the classical versions of these equations are recovered.

3 Gradient elastic flexural stiffness matrix

This section deals with the development of the stiffness matrix of a gradient elastic flexural beam element with two nodes 1 and 2 at its two ends, as shown in Fig. 3. On the basis of Eq. (4) describing the boundary conditions of the problem, one concludes that there are three nodal generalized displacements (v, v', v'') and three nodal generalized forces (V, M, m) associated with those displacements at every node, as shown in Fig. 3. In other words, every node has three degrees of freedom (d.o.f.): displacement, slope and curvature. These nodal generalized displacements and forces of Fig. 3 are considered to be positive. One can observe that the positive nodal quantities of Fig. 3 (matrix convention) are not the same with the corresponding ones of Fig. 2 (mechanics convention), and this fact has to be taken into account when transferring information from one figure to the other.

For the construction of the stiffness matrix of the finite element of Fig. 3, one needs to select a displacement function and adopt a definition of that matrix. In this work, the displacement function is selected to be the exact solution of the homogeneous part of Eq. (3), which has the form [11]

$$v(x) = C_1 x^3 + C_2 x^2 + C_3 x + C_4 + C_5 g^4 \sinh(x/g) + C_6 g^4 \cosh(x/g), \tag{7}$$

where $C_1, C_2, \ldots, C_6$ are constants of integration to be determined. It is observed that in the limit as $g \to 0$, the above displacement function reduces to the cubic polynomial used in classical finite element analysis. Because use is made of the exact solution of the governing equation of the problem as the displacement function, it is

expected that the stiffness matrix to be constructed will be exact, and hence, the response of a beam structure to static loading analyzed on the basis of the FEM with that element stiffness matrix for every physical member will be also exact.

The stiffness matrix of the finite element of Fig. 3 will be constructed here on the basis of the displacement function (7) and the basic definition of any coefficient of that matrix. Thus, for a stiffness matrix $[K]$ connecting the vector of generalized nodal forces {F} with the vector {U} of the corresponding nodal displacements as

$$\{F\} = [K]\{U\}, \tag{8}$$

the stiffness coefficient K_{ij} is defined as the nodal generalized force at the degree of freedom i due to a unit nodal generalized displacement of the degree of freedom j, while all the other displacements are zero. In this work, since every node has 3 d.o.f., the finite element of Fig. 3 has $2 \times 3 = 6$ d.o.f., and hence, the size of the stiffness matrix $[K]$ will be 6×6, while the indices i, j will take the values $1, 2, \ldots, 6$. Thus, the stiffness matrix will be constructed here column by column on the basis of six generalized displacements states, the displacement function (7) and the expressions for V, M, m in terms of that displacement and its derivatives as defined in Eq. (4).

Thus, the derivatives of $v = v(x)$ of Eq. (7) are evaluated and listed as

$$\begin{aligned}
v'(x) &= 3C_1x^2 + 2C_2x + C_3 + C_5g^3\cosh(x/g) + C_6g^3\sinh(x/g),\\
v''(x) &= 6C_1x + 2C_2 + C_5g^2\sinh(x/g) + C_6g^2\cosh(x/g),\\
v'''(x) &= 6C_1 + C_5g\cosh(x/g) + C_6g\sinh(x/g),\\
v^{\mathrm{IV}}(x) &= C_5\sinh(x/g) + C_6\cosh(x/g),\\
v^{\mathrm{V}}(x) &= C_5(1/g)\cosh(x/g) + C_6(1/g)\sinh(x/g),
\end{aligned} \tag{9}$$

while the generalized forces V, M and m are expressed in terms of the above derivatives with the aid of Eq. (4) as

$$\begin{aligned}
V(x) &= \mathrm{EI}\left(v'' - g^2v^{\mathrm{V}}\right),\\
M(x) &= \mathrm{EI}\left(v'' - g^2v^{\mathrm{IV}}\right),\\
m(x) &= \mathrm{EI}g^2v'''.
\end{aligned} \tag{10}$$

Consider the first displacement state defined as

$$\begin{aligned}
v(0) = \quad & v_1 = 1, \quad v'(0) = v_1' = 0, \quad v''(0) = v_1'' = 0,\\
v(L) = \quad & v_2 = 0, \quad v'(L) = v_2' = 0, \quad v''(L) = v_2'' = 0,
\end{aligned} \tag{11}$$

where v_1, v_1', v_1'', v_2, v_2', v_2'' are the generalized nodal displacements of the finite element of Fig. 3. The above Eq. (11) in view of the expressions (9) can be written in the form

$$\begin{aligned}
&C_4 + C_6g^4 = 1, \quad C_3 + C_5g^3 = 0, \quad 2C_2 + C_6g^2 = 0,\\
&C_1L^3 + C_2L^2 + C_3L + C_4 + C_5g^4\sinh(L/g) + C_6g^4\cosh(L/g) = 0,\\
&3C_1L^2 + 2C_2L + C_3 + C_5g^3\cosh(L/g) + C_6g^3\sinh(L/g) = 0,\\
&6C_1L + 2C_2 + C_5g^2\sinh(L/g) + C_6g^2\cosh(L/g) = 0.
\end{aligned} \tag{12}$$

The above Eq. (12) can be thought of as a system of six equations with six unknowns, the constants $C_i (i = 1, 2, \ldots, 6)$ and easily solved to provide

$$\begin{aligned}
C_1 &= \frac{2}{12g^2L + L^3 - 6gL^2\coth[\frac{L}{2g}]},\\
C_2 &= -\frac{3}{12g^2 + L^2 - 6gL\coth[\frac{L}{2g}]},\\
C_3 &= \frac{6g}{-6gL + (12g^2 + L^2)\tanh[\frac{L}{2g}]},
\end{aligned} \tag{13}$$

$$C_4 = 1 - \frac{6g^2}{12g^2 + L^2 - 6gL\coth[\frac{L}{2g}]},$$
$$C_5 = \frac{1}{g^3 L - \frac{1}{6}g^2(12g^2 + L^2)\tanh[\frac{L}{2g}]},$$
$$C_6 = \frac{6}{g^2\left(12g^2 + L^2 - 6gL\coth\left[\frac{L}{2g}\right]\right)}.$$

Using the definition of the stiffness coefficients K_{ij} and the different sign convention of Fig. 2 (mechanics convention) and Fig. 3 (matrix convention), one can obtain the K_{ij} stiffness coefficients for the first column of $[K]$ corresponding to displacement state (11) in the form

$$\begin{aligned} &K_{11} = V(0), \quad K_{21} = M(0), \quad K_{31} = m(0), \\ &K_{41} = -V(L), \quad K_{51} = -M(L), \quad K_{61} = -m(L), \end{aligned} \tag{14}$$

where the right-hand sides of Eq. (14) can be computed by using Eqs. (10) and (9) with values for the constants $C_i (i = 1, 2, \ldots, 6)$ those of Eq. (13). Thus, the above stiffness coefficients K_{ij} of Eq. (14) can be written explicitly in the form:

$$\begin{aligned} K_{11} &= \frac{12\mathrm{EI}}{12g^2L + L^3 - 6gL^2\coth\left[\frac{L}{2g}\right]}, \\ K_{21} &= -\frac{6\mathrm{EI}}{12g^2 + L^2 - 6gL\coth\left[\frac{L}{2g}\right]}, \\ K_{31} &= \mathrm{EI}\left(\frac{1}{L} - \frac{L}{12g^2 + L^2 - 6gL\coth\left[\frac{L}{2g}\right]}\right), \\ K_{41} &= -\frac{12\mathrm{EI}}{12g^2L + L^3 - 6gL^2\coth\left[\frac{L}{2g}\right]}, \\ K_{51} &= -\frac{6\mathrm{EI}}{12g^2 + L^2 - 6gL\coth\left[\frac{L}{2g}\right]}, \\ K_{61} &= \mathrm{EI}\left(-\frac{1}{L} + \frac{L}{12g^2 + L^2 - 6gL\coth\left[\frac{L}{2g}\right]}\right). \end{aligned} \tag{15}$$

Consider now the second displacement state defined as

$$\begin{aligned} &v'(0) = v_1' = 1, \quad v(0) = v_1 = 0, \quad v''(0) = v_1'' = 0, \\ &v(L) = v_2 = 0, \quad v'(L) = v_2' = 0, \quad v''(L) = v_2'' = 0. \end{aligned} \tag{16}$$

The above Eq. (16) in view of the expressions (9) can be written as a system of six linear equations with six unknown coefficients $C_i (i = 1, 2, \ldots, 6)$, which can be solved and provide explicit expressions for the six coefficients C_i. Using the definition of the stiffness coefficients K_{ij} and the different sign convention in Figs. 2 and 3, one can obtain the K_{ij} stiffness coefficients for the second column of $[K]$ corresponding to the displacement state (16) in the form

$$\begin{aligned} &K_{12} = V(0), \quad K_{22} = M(0), \quad K_{32} = m(0), \\ &K_{42} = -V(L), \quad K_{52} = -M(L), \quad K_{62} = -m(L), \end{aligned} \tag{17}$$

where the right-hand sides of Eq. (17) can be computed by using Eqs. (10) and (9) with values for the constants C_i (i = 1, 2, …, 6) those obtained for the present second displacement state.

The above procedure is repeated in exactly the same way for the other four remaining displacement states identified by $v''(0) = v_1'' = 1$, $v(L) = v_2 = 1$, $v'(L) = v_2'(L) = 1$, $v''(L) = v_2'' = 1$, and the four remaining

columns of the stiffness matrix $[K]$ are explicitly derived in closed form. Due to the symmetry of the matrix $[K]$, the satisfaction of the relation $K_{ij} = K_{ji}$ serves as a verification of the exactness of these expressions for K_{ij}. Thus, the stiffness equation (8) connecting the vectors $\{F\}$ and $\{U\}$ through the stiffness matrix $[K]$ for the finite element of Fig. 3 can be explicitly written down with

$$\begin{aligned} \{F\} &= \{V_1, M_1, m_1, \quad V_2, M_2, m_2\}^{\mathrm{T}}, \\ \{U\} &= \left\{v_1, v_1', \quad v_1'', v_2, \quad v_2', \quad v_2''\right\}^{\mathrm{T}}, \end{aligned} \tag{18}$$

and the various elements K_{ij} of the matrix $[K]$ given in Appendix 1. One can prove through a limiting process that for $g = 0$, the expressions for the K_{ij} stiffness coefficients reduce to the classical ones found, e.g., in [19].

Figure 4a–f depicts the deflection $v = v(\xi)$ versus $\xi = x/L$ for four values of $g/L(0.001, 0.03, 0.06, 0.1)$ for the six displacement states ($v_1 = 1$, $v_1' = 1$, $v_1'' = 1$, $v_2 = 1$, $v_2' = 1$, $v_2'' = 1$) used to derive the six columns of the stiffness matrix $[K]$, respectively. It is observed that Fig. 4a and d, b and e, c and f are mirror images of each other, as expected. Furthermore, it is observed that in Fig. 4a and d, v increases for increasing g/L up to $\xi = 0.5$, while this behavior is reversed for $0.5 < \xi < 1.0$. A similar behavior is observed in Fig. 4b and e but with the inflection point being now $\xi = 0.65$ (for Fig. 4b) and $\xi = 0.45$ (for Fig. 4e). Finally, it is observed that Fig. 4c and f shows an increase of v for increasing g/L without any clearly visible inflection point.

4 The case of distributed loading

In the FEM, the load on any element is assumed to be nodal. Thus, in case the load is distributed, it has to be replaced by equivalent nodal load. An approximate way of determining this equivalent load is to divide the element into a number of subelements and substitute the distributed load of every subelement by two vertical nodal forces, which are equal and opposite to the reactions of the corresponding, to this subelement, simply supported beam under that distributed load. However, this approximate method requires a large number of subelements for acceptable accuracy and is not compatible with the "exact" FEM presented in the previous section.

For this reason, the equivalent to the distributed load nodal loads are determined so as to produce the same deformation as the distributed load. This implies that these equivalent nodal loads are equal and opposite to the end reactions of the beam element fixed at both of its ends under the distributed load. This approach is an "exact" one. In the following, these equivalent nodal loads will be determined for the simple case of uniformly distributed load, which is the most frequently occurred case in practice.

Consider the fixed–fixed uniform beam of length L, flexural rigidity EI and gradient coefficient g under the action of a uniformly distributed vertical load q, as shown in Fig. 5. The solution of Eq. (3), which governs the behavior of this beam, is given as the sum of the solution of its homogeneous part provided by Eq. (7), plus the particular solution $-qx^4/24EI$, i.e., as

$$v(x) = C_1x^3 + C_2x^2 + C_3x + C_4 + C_5g^4\sinh(x/g) + C_6g^4\cosh(x/g) - (qx^4/24EI). \tag{19}$$

On the basis of Eq. (19), one can obtain the derivatives

$$\begin{aligned} v'(x) &= 3C_1x^2 + 2C_2x + C_3 + C_5g^3\cosh(x/g) + C_6g^3\sinh(x/g) - \left(qx^3/6EI\right), \\ v''(x) &= 6C_1x + 2C_2 + C_5g^2\sinh(x/g) + C_6g^2\cosh(x/g) - \left(qx^2/2EI\right), \\ v'''(x) &= 6C_1 + C_5g\cosh(x/g) + C_6g\sinh(x/g) - (qx/EI), \\ v^{\mathrm{IV}}(x) &= C_5\sinh(x/g) + C_6\cosh(x/g) - (q/EI), \\ v^{\mathrm{V}}(x) &= C_5(1/g)\cosh(x/g) + C_6(1/g)\ \sinh(x/g). \end{aligned} \tag{20}$$

Because of symmetry with respect to geometry and loading, one can consider only half of the beam and write the boundary conditions in the form

$$\begin{aligned} v(0) = v'(0) = v''(0) = 0, \\ v'(L/2) = v''(L/2) = V(L/2) = 0, \end{aligned} \tag{21}$$

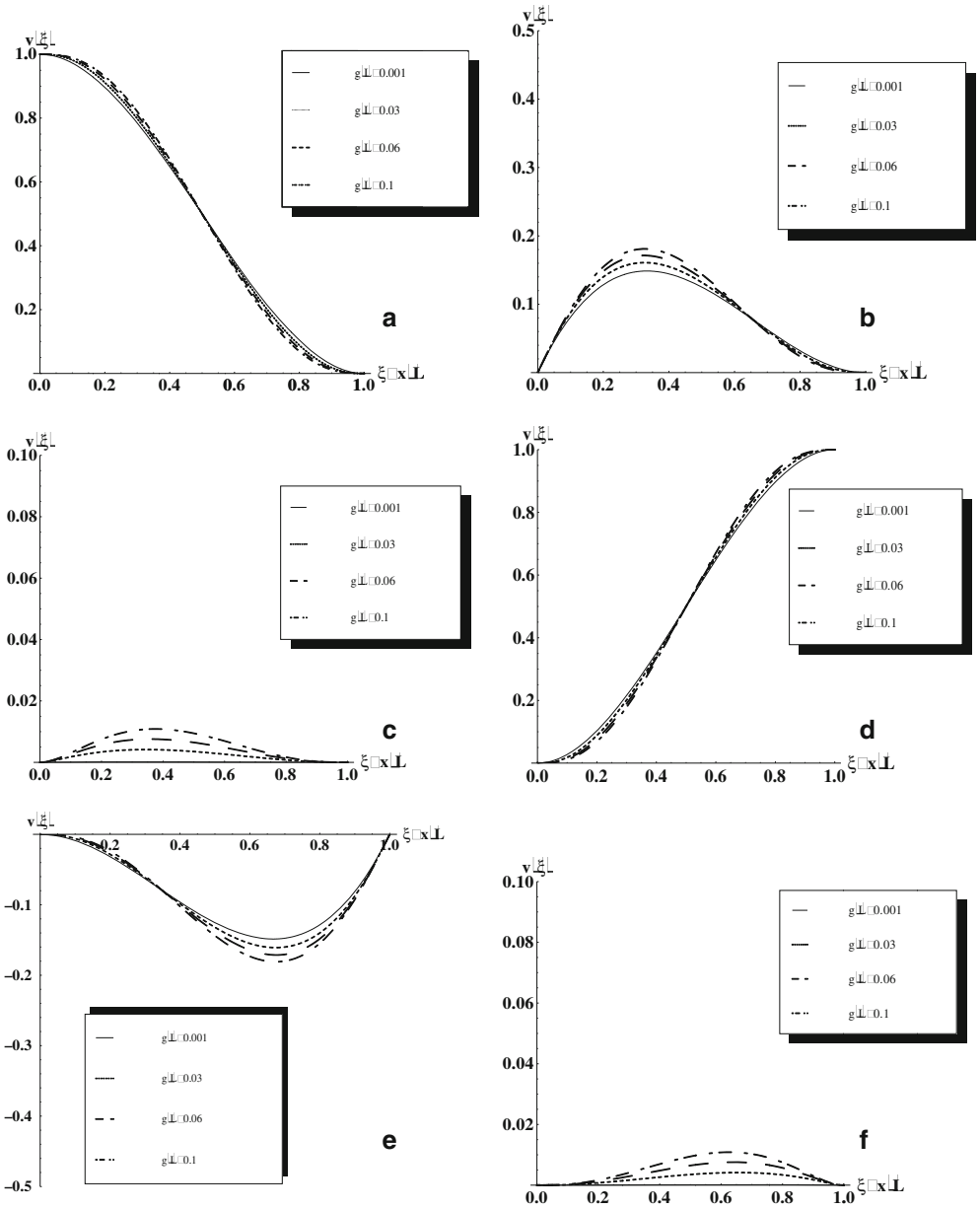

Fig. 4 Deflection $v(\xi)$ versus $\xi = x/L$ for various values of g/L for the six displacement states of a gradient elastic beam element

where $V(x)$ is expressed in terms of $v'''(x)$ and $v^{v}(x)$ as shown in Eq. $(10)_1$. Using Eq. (20), one can write Eq. (21) in the form

$$\begin{gathered} C_4 + C_6 g^4 = 0, \qquad C_3 + C_5 g^3 = 0, \qquad 2C_2 + C_6 g^2 = 0, \\ 3C_1 (L/2)^2 + 2C_2 (L/2) + C_3 + C_5 g^3 \cosh(L/2g) + C_6 g^3 \sinh(L/2g) = q (L/2)^3 / 6\mathrm{EI}, \\ 6C_1 (L/2) + 2C_2 + C_5 g^2 \sinh(L/2g) + C_6 g^2 \cosh(L/2g) = qL^2/8\mathrm{EI}, \\ 6C_1 = qL/2\mathrm{EI}. \end{gathered} \tag{22}$$

The above system of equations is analytically solved with the aid of Mathematica [23] and yields

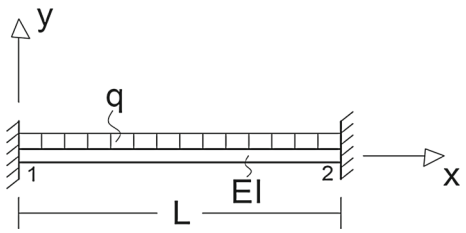

Fig. 5 A fixed–fixed gradient elastic beam under uniformly distributed vertical load q

$$
\begin{aligned}
C_1 &= \frac{Lq}{12\mathrm{EI}},\\
C_2 &= \frac{qL^2\left(3g\sinh\left[\frac{L}{4g}\right]-L\cosh\left[\frac{L}{4g}\right]\right)}{24\mathrm{EI}\left(L\cosh\left[\frac{L}{4g}\right]-4g\sinh\left[\frac{L}{4g}\right]\right)},\\
C_3 &= \frac{gL^2q\,\mathrm{csch}\left[\frac{L}{4g}\right]\left(-L-2L\cosh\left[\frac{L}{2g}\right]+6\sinh\left[\frac{L}{2g}\right]\right)}{48\mathrm{EI}(-L\cosh[\frac{L}{4g}]+4g\sinh[\frac{L}{4g}])},\\
C_4 &= \frac{g^2L^2q\left(-L\cosh\left[\frac{L}{4g}\right]+3g\sinh\left[\frac{L}{4g}\right]\right)}{12\mathrm{EI}\left(L\cosh\left[\frac{L}{4g}\right]-4g\sinh\left[\frac{L}{4g}\right]\right)},\\
C_5 &= q\,\mathrm{csch}\left[\frac{L}{2g}\right]^2\frac{\left(-6gL^2\cosh\left[\frac{L}{4g}\right]+3gL^2\cosh\left[\frac{3L}{4g}\right]+3gL^2\cosh\left[\frac{5L}{4g}\right]-L^3\sinh\left[\frac{L}{4g}\right]-2L^3\sinh\left[\frac{3L}{4g}\right]\right)}{48g^2\mathrm{EI}\left(-L\cosh\left[\frac{L}{4g}\right]+4g\sinh\left[\frac{L}{4g}\right]\right)},\\
C_6 &= \frac{L^3q\cosh\left[\frac{L}{4g}\right]-3gL^2q\sinh\left[\frac{L}{4g}\right]}{12Eg^2IL\cosh\left[\frac{L}{4g}\right]-48Eg^3I\sinh}\left[\frac{L}{4g}\right].
\end{aligned}
\tag{23}
$$

Use of Eq. (10) in conjunction with Eqs. (20) and (23) enables one to obtain the reactions at x=0 in the form

$$
\begin{aligned}
V(0) &= \frac{Lq}{2},\\
M(0) &= \frac{1}{48}q\left(48g^2+L^2\left(-3-\frac{L}{L-4g\tanh\left[\frac{L}{4g}\right]}\right)\right),\\
m(0) &= \frac{1}{48}gLq\left(24g-3L\coth\left[\frac{L}{4g}\right]+\frac{L^2}{4g-L\coth\left[\frac{L}{4g}\right]}\right).
\end{aligned}
\tag{24}
$$

It is observed that for $g = 0$, one can recover from (24) the classical values of $V = qL/2, M(0) = -qL^2/12, m(0) = 0$. The above expressions (24) together with $V(L) = V(0), M(L) = -M(0), m(L) = m(0)$ and with the opposite signs can be used as nodal loads equivalent to a uniformly distributed load q on a beam element.

5 Gradient elastic stability stiffness matrix

This section deals with the development of the stiffness matrix of a gradient elastic flexural beam element subjected to a constant compressive axial load P and having two nodes 1 and 2 at its two ends, as shown in Fig. 6. The generalized nodal forces and nodal displacements shown in Fig. 6 are the same as those in Fig. 3 for the simple flexural beam element. However, in this case, the axial load P creates second-order moments and the governing equation is Eq. (5) instead of Eq. (3).

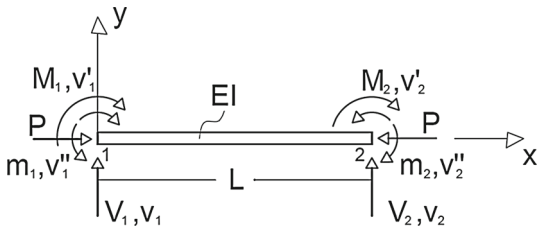

Fig. 6 Matrix convention for generalized nodal forces and displacements of a gradient elastic flexural beam element with a constant compressive axial force

For the construction of the stability stiffness matrix $[S]$ of the finite element of Fig. 6, the displacement function is selected to be the exact solution of Eq. (5), which has the form [11]

$$v(x) = C_1 x + C_2 + C_3 \sin\xi x + C_4 \cos\xi x + C_5 \sinh\theta x + C_6 \cosh\theta x, \tag{25}$$

where

$$\xi = \left(\frac{1}{\sqrt{2}g}\right)\sqrt{\sqrt{1+4g^2k^2}-1},$$
$$\theta = \left(\frac{1}{\sqrt{2}g}\right)\sqrt{1+\sqrt{1+4g^2k^2}},$$
$$k^2 = \frac{P}{\mathrm{EI}}, \tag{26}$$

and $C_1, C_2, \ldots, C_6$ are constants of integration to be determined. It is observed that in the limit as $P \to 0$, the above displacement function reduces to that of Eq. (7) and as $P \to 0$ and $g \to 0$ to the classical cubic polynomial. Because use is made of the exact solution of the governing equation of the problem as the displacement function, as in the previous section, it is expected that the matrix $[S]$ to be exact and the buckling load of the beam structure obtained by using this matrix to be also exact.

Following exactly the same procedure as in the previous section, one can obtain the stability stiffness equation

$$\{F\} = [S]\{U\}, \tag{27}$$

where the vectors $\{F\}$ and $\{U\}$ are given again by Eq. (18), while the elements S_{ij} of the stability stiffness matrix $[S]$ are given in Appendix 2. It should be noticed that all the entries of matrix $[S]$ are complicated functions of P, which in the limit, as $P \to 0$, reduce to the flexural stiffness coefficients K_{ij} of Appendix 1. In case the axial load P is tensile, one can use the aforementioned coefficients S_{ij} but with $-P$ instead of P. This creates minus signs under square roots and use should be made of complex arithmetic. Of course, one could also modify analytically the expressions for S_{ij} of Appendix 2 for this case of tensile load and derive real-valued expressions as in the classical case but this would be very complicated and is not recommended.

6 Numerical examples

Seven examples are presented in this section to illustrate the use of the previously developed stiffness matrices in the framework of the FEM and demonstrate the advantages of the whole procedure when one has to determine the response of gradient elastic beam structures to static loading. Five examples deal with the analysis of statically determinate and indeterminate beams of uniform and nonuniform cross-section and two examples with determination of the buckling load of a beam under different types of nonclassical boundary conditions.

Example 1 Consider a gradient elastic uniform cantilever beam of length L and flexural rigidity EI subjected to a vertical lateral concentrated load P at its free end, as shown in Fig. 7. The vertical deflection at the loaded free end of this beam will be determined by the FEM.

The whole beam is considered to be one finite element with nodes 1 and 2 at the fixed and free ends, respectively, as shown in Fig. 7. The static behavior of a beam element 1–2 is described by the stiffness

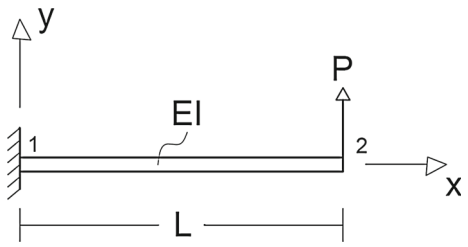

Fig. 7 Geometry and loading of a cantilever gradient elastic flexural beam

equation (8) with the force and displacements vectors $\{F\}$ and $\{U\}$ as given by Eq. (18) and the entries of the stiffness matrix $[K]$ as given in Appendix 1.

The boundary conditions of the problem in terms of generalized nodal displacements are

$$v_1 = v_1' = v_1'' = 0 \tag{28}$$

with the first two conditions in (28) being the classical and the third condition the nonclassical ones. These conditions, on account of Eq. (10), indicate large V and very small M and m. On the other hand, if one assumes $v_1 = v_1' = m = 0$ instead of (28), which are acceptable boundary conditions in view of Eq. (4), M is large, V is very small and $m = 0$. Thus, one can observe some peculiarities of the theory concerning the magnitudes of M and V at the fixed end of the beam. On the basis of Eq. (28), the matrix equation (8) takes the form

$$\begin{Bmatrix} P \\ 0 \\ 0 \end{Bmatrix} = \begin{bmatrix} K_{44} & K_{45} & K_{46} \\ K_{54} & K_{55} & K_{56} \\ K_{64} & K_{65} & K_{66} \end{bmatrix} \begin{Bmatrix} v_2 \\ v_2' \\ v_2'' \end{Bmatrix}. \tag{29}$$

The above matrix equation with K_{ij} as explicitly given in Appendix 1 is solved analytically with the aid of Mathematica [23], and the unknown nodal displacements v_2, v_2' and v_2'' are explicitly determined as

$$\begin{aligned} v_2 &= \frac{PL^3}{3\mathrm{EI}}\left[1 + 3\left(\frac{g}{L}\right)^2 - 6\left(\frac{g}{L}\right)^2 \operatorname{sech}\left(\frac{L}{g}\right) + 3\left(\frac{g}{L}\right)^3 \tanh\left(\frac{L}{g}\right) - 3\left(\frac{g}{L}\right)\tanh\left(\frac{L}{g}\right)\right], \\ v_2' &= \frac{P\left(-2g^2 - L^2 + 2g\operatorname{sech}\left(\frac{L}{g}\right)\left(g + L\sinh\left(\frac{L}{g}\right)\right)\right)}{2\mathrm{EI}}, \\ v_2'' &= \frac{P\operatorname{sech}\left(\frac{L}{g}\right)\left(L - g\sinh\left(\frac{L}{g}\right)\right)}{\mathrm{EI}}. \end{aligned} \tag{30}$$

Once these are known, the reactions V_1, M_1 and m_1 at node 1, corresponding to zero generalized displacements, are easily determined from Eq. (8).

The expression for the deflection v_2 in (30), after some manipulations, can be written in the form

$$\begin{aligned} v_2 = \frac{PL^3}{3\mathrm{EI}}&\left[1 - 3\left(\frac{g}{L}\right)^2\left[\cosh\left(\frac{L}{g}\right) + \frac{1}{\cosh\left(\frac{L}{g}\right)} + \left(\frac{L}{g}\right)\tanh\left(\frac{L}{g}\right) - 1\right]\right] \\ &+ \frac{PL^3}{3\mathrm{EI}}\left[3\left(\frac{g}{L}\right)^3\left[\tanh\left(\frac{L}{g}\right) + \left(\frac{L}{g}\right)\sinh\left(\frac{L}{g}\right)\tanh\left(\frac{L}{g}\right)\right]\right], \end{aligned}$$

which is exactly the same as the deflection obtained in [14] by an analytic approach. Figure 8 depicts the normalized deflection v_2/v_2^c, where $v_2^c = PL^3/3\mathrm{EI}$ is the classical one, versus g/L. From this figure, one can easily observe the decrease of the deflection v_2 for increasing values of the gradient coefficient g (stiffening effect in gradient elasticity).

Example 2 Consider a simply supported gradient elastic beam of length $2L$ and flexural rigidity EI under a lateral concentrated vertical load P at the middle of its span, as shown in Fig. 9. The above beam is considered as a beam structure composed of two finite elements 1–2 and 2–3, as shown in Fig. 9. With 3 d.o.f. per node, the whole beam has $3 \times 3 = 9$ d.o.f., and hence, the total structural stiffness matrix will be of the order of

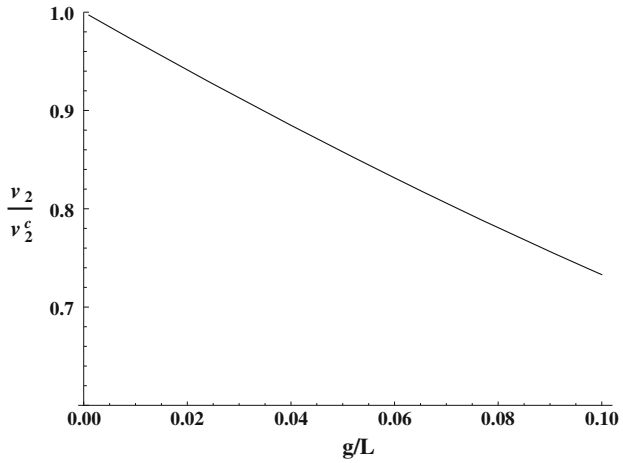

Fig. 8 Deflection versus g/L of the cantilever gradient elastic beam of Fig. 7

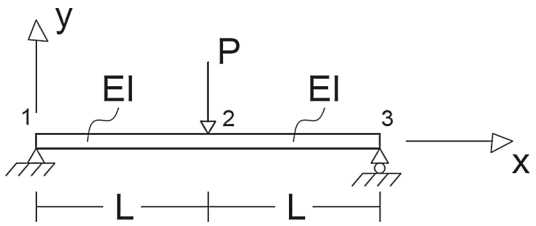

Fig. 9 Geometry and loading of a simply supported gradient elastic flexural beam

9×9. This stiffness matrix is obtained by a simple superposition of the stiffness matrices 6×6 of the finite elements 1–2 and 2–3 as given by Eq. (8) by following standard procedures [19].

The classical boundary conditions of the problem in terms of generalized nodal displacements are

$$v_1 = v_3 = v_2' = 0, \tag{31}$$

where the third boundary condition in (31) comes from symmetry considerations. The nonclassical boundary conditions are assumed to be

$$v_1'' = v_3'' = 0. \tag{32}$$

Thus, the total structural stiffness matrix of order 9×9, due to the 5 boundary conditions (31) and (32), becomes 4×4, and the stiffness equation takes the form (8) with

$$\begin{aligned} \{F\} &= \{0, -P, 0, 0\}^{\mathrm{T}}, \\ \{U\} &= \left\{v_1', v_2, v_2'', v_3'\right\}^{\mathrm{T}}. \end{aligned} \tag{33}$$

The above system of 4 equations with 4 unknowns is solved analytically with the aid of Mathematica [23], and the result is

$$\begin{aligned} v_1' &= \left(\frac{P}{4\mathrm{EI}}\right)\left[-2g^2 + L^2 + 2g^2 \mathrm{sech}\left(\frac{L}{g}\right)\right], \\ v_2 &= \left(-\frac{P}{6\mathrm{EI}}\right)\left[-3g^2 L + L^3 + 3g^3 \tanh\left(\frac{L}{g}\right)\right], \\ v_2'' &= \left(-\frac{P}{2\mathrm{EI}}\right)\left[L - g \tanh\left(\frac{L}{g}\right)\right], \\ v_3' &= \left(-\frac{P}{4\mathrm{EI}}\right)\left[-2g^2 + L^2 + 2g^2 \mathrm{sech}\left(\frac{L}{g}\right)\right]. \end{aligned} \tag{34}$$

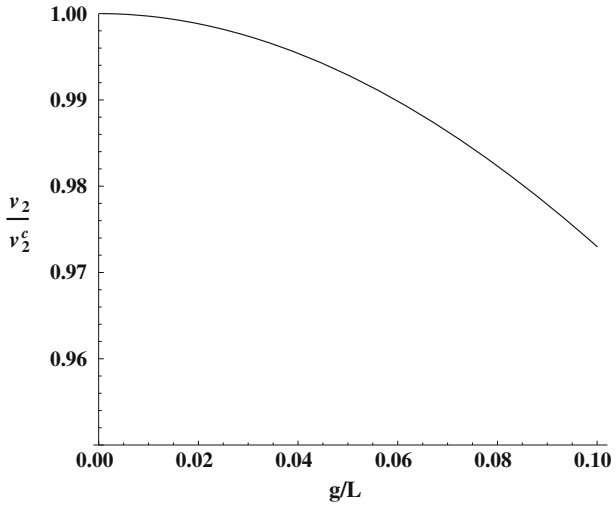

Fig. 10 Deflection versus g/L of the simply supported gradient elastic beam of Fig. 9

With the known displacements in (34), one can easily determine the reactions V_1, V_3, m_1 and m_3 corresponding to zero generalized displacements. Figure 10 depicts the normalized deflection v_2/v_2^c, where $v_2^c = -PL^3/6\text{EI}$ is the classical one, versus g/L. From this figure, one can easily observe the decrease of the deflection v_2 for increasing values of the gradient coefficient g (stiffening effect in gradient elasticity).

For verification reasons, the same problem was also solved analytically. To this end, half of the beam was considered for the analysis by taking advantage of symmetry. For this structure, the deflection $v(x)$ is given by Eq. (7) and one essentially has to determine the integration constants C_1, C_2,…,C_6. The classical boundary conditions of the problem are

$$\begin{aligned} v(0) &= 0, \quad v'(L) = 0, \\ M(0) &= 0, \quad V(L) = -P/2, \end{aligned} \tag{35}$$

while the nonclassical ones are assumed to be

$$v''(0) = 0, \quad m(L) = 0. \tag{36}$$

The above 6 boundary conditions are written explicitly with the aid of Eq. (9) providing the derivatives of $v(x)$ and (10) providing expressions of $V(x)$, $M(x)$ and $m(x)$ in terms of derivatives of $v(x)$. Thus, a linear system of 6 equations with 6 unknowns [the constants C_1, C_2,…, C_6 in (7)] is created and solved with the aid of Mathematica [22]. The explicit expressions for these constants are given as

$$\begin{aligned} &C_1 = -P/12\text{EI}, \quad C_2 = 0, \quad C_3 = -\left(P/4\text{EI}\right)\left(2g^2 - L^2\right), \\ &C_4 = 0, \quad C_5 = \left(P/2g\text{EI}\right)\operatorname{sech}\left(L/g\right), \quad C_6 = 0. \end{aligned} \tag{37}$$

Once these constants are known, $v(x)$ and its derivatives become also known. Thus, $v'(0)$, $v(L)$ and v''(L) can be easily evaluated and take exactly the form of v_1', v_2 and v_2'', respectively, given in Eq. (34) thereby verifying the results of the finite element analysis.

Example 3 Consider a gradient elastic beam structure composed of two members with different cross-sections fixed at one end and on rollers at the other end and subjected to a vertical lateral concentrated load P at the middle of its span, as shown in Fig. 11. The flexural rigidities of the two members I and II of Fig. 11 are EI_1 and EI_2, respectively, with $I_1 = 2I_2 = 2I$, while their lengths are equal to L. This structure is modeled by two finite elements 1–2 and 2–3 and has 3 nodes with 3 d.o.f. per node, as shown in Fig. 11. Thus, the total structural stiffness matrix resulting from the superposition of the stiffness matrices of its two elements is 9×9. The classical boundary conditions of this problem in terms of generalized nodal displacements are

$$v_1 = v_1' = v_3 = 0, \tag{38}$$

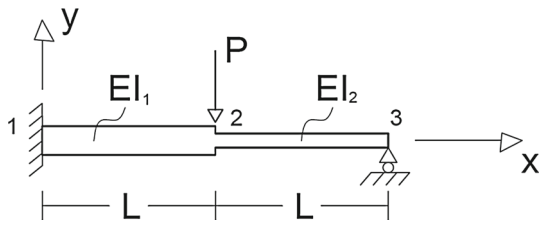

Fig. 11 Geometry and loading of a fixed-hinged gradient elastic beam composed of two members with different cross-sections

while it is assumed that there is only one nonclassical boundary condition of the form

$$v_1'' = 0. \tag{39}$$

Application of these 4 boundary conditions in the stiffness equation for the whole structure results in a reduced in size stiffness equation, i.e., in a system of 5 equations with 5 unknown generalized displacements v_2, v_2', v_2'', v_3', v_3'' and a generalized force vector $\{F\} = \{-P, 0, 0, 0, 0\}^{\mathrm{T}}$.

This system of equations is solved analytically with the aid of Mathematica [23] and yields the unknowns v_2, v_2', v_2'', v_3'andv_3''. The expressions for these unknowns are very lengthy, and for this reason, only v_2 and v_3' are given below for illustration purposes:

$$\begin{aligned} v_2 = \big(&P\left(144g^6 - 504g^4L^2 - 96g^2L^4 - 11L^6 + 96g^2L^2\left(-6g^2 + 5L^2\right)\cosh[L/g]\right.\\ &-3\left(48g^6 - 264g^4L^2 + 16g^2L^4 + 11L^6\right)\cosh[2L/g]\\ &+24gL\left(-\left(-60g^4 + 8g^2L^2 + L^4\right)\sinh[L/g]\right.\\ &\left.\left.+\left(-18g^4 - 21g^2L^2 + 5L^4\right)\sinh[2L/g]\right)\right) / \left(72\mathrm{EI}\left(-8g^2L\cosh[L/g] + 9L\left(g^2 + L^2\right)\cosh[2L/g]\right.\right.\\ &\left.\left.+L\left(-13g^2 + 3L^2 - 8gL\sinh[L/g]\right) + g\left(6g^2 - 13L^2\right)\sinh[2L/g]\right)\right), \end{aligned} \tag{40}$$

$$\begin{aligned} v_3' = \big(&P\left(44g^2L^3 - 7L^5 + \left(96g^4L + 88g^2L^3\right)\cosh[L/g]\right.\\ &-3L\left(32g^4 + 28g^2L^2 + 7L^4\right)\cosh[2L/g] - 24g^3\left(8g^2 + 5L^2\right)\sinh[L/g]\\ &\left.+4g\left(24g^4 + 15g^2L^2 + 16L^4\right)\sinh[2L/g]\right) / \left(24\mathrm{EI}\left(-8g^2L\cosh[L/g]\right.\right.\\ &+9L\left(g^2 + L^2\right)\cosh[2L/g] + L\left(-13g^2 + 3L^2 - 8gL\sinh[L/g]\right)\\ &\left.\left.+g\left(6g^2 - 13L^2\right)\sinh[2L/g]\right)\right). \end{aligned} \tag{41}$$

Once the nodal generalized displacements have been found, one can easily determine the generalized nodal reaction forces V_1, M_1, V_3, and m_1 corresponding to zero generalized nodal displacements. Just as an example, the reaction V_1 has the explicit form

$$\begin{aligned} V_1 = \big(&P\left(-60g^2L + 13L^3 + 3L\left(4g^2 + 13L^2\right)\cosh[2L/g]\right.\\ &\left.-12g\left(2g^2 + 3L^2\right)\sinh[L/g] + 6g\left(6g^2 - 7L^2\right)\sinh[2L/g]\right) / \left(6\left(-8g^2L\cosh[L/g]\right.\right.\\ &+9L\left(g^2 + L^2\right)\cosh[2L/g] + L\left(-13g^2 + 3L^2 - 8gL\sinh[L/g]\right)\\ &\left.\left.+g\left(6g^2 - 13L^2\right)\sinh[2L/g]\right)\right). \end{aligned} \tag{42}$$

For verification reasons, the same problem was also solved analytically but only for its classical version since its gradient elastic version is very complicated to be solved analytically. This example clearly demonstrates the usefulness of the FEM for solving complicated gradient elastic problems like the present one characterized by static indeterminancy and variable cross-sections.

Consider the classical elastic structure of Fig. 12 under the load P and the reactions at its supports, M_{A}, R_{A} and R_{C}. The equilibrium equations for this structure read

$$\begin{aligned} &R_{\mathrm{A}} + R_{\mathrm{C}} - P = 0,\\ &M_{\mathrm{A}} - R_{\mathrm{C}}2L + PL = 0, \end{aligned} \tag{43}$$

while its boundary conditions have the form

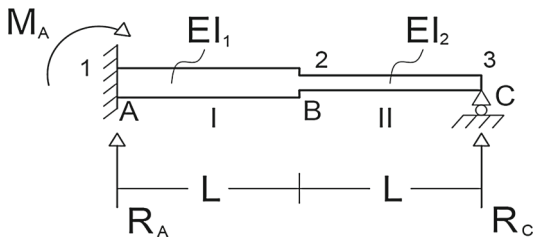

Fig. 12 Geometry, loading and reaction forces and moments of the elastic beam structure of Fig. 11

$$\begin{aligned} v_{\mathrm{I}}(0) &= v_{\mathrm{I}}'(0) = 0, \\ v_{\mathrm{II}}(2L) &= 0, \end{aligned} \tag{44}$$

where the subscripts I and II refer to the members AB and BC, respectively. In addition, one has the compatibility equations at B in the form

$$\begin{aligned} v_{\mathrm{I}}(L) &= v_{\mathrm{II}}(L), \\ v_{\mathrm{I}}'(L) &= v_{\mathrm{II}}'(L). \end{aligned} \tag{45}$$

For the parts I and II of the structure, one has the equations

$$\begin{aligned} \mathrm{EI}_1 \left(\frac{\partial^2 v_I}{\partial x^2} \right) &= M_{\mathrm{A}} + R_{\mathrm{A}} x \qquad 0 \le x \le L, \\ \mathrm{EI}_2 \left(\frac{\partial^2 v_{II}}{\partial x^2} \right) &= M_{\mathrm{A}} + R_{\mathrm{A}} x - P\,(x - L) \qquad L \le x \le 2L, \end{aligned} \tag{46}$$

which after integration yield

$$\begin{aligned} v_I'(x) &= \frac{1}{\mathrm{EI}_1} \left(M_{\mathrm{A}} x + R_{\mathrm{A}} \frac{x^2}{2} + G_1 \right), \\ v_I(x) &= \frac{1}{\mathrm{EI}_1} \left(M_{\mathrm{A}} \frac{x^2}{2} + R_{\mathrm{A}} \frac{x^3}{6} + G_1 x + G_2 \right), \\ v_{II}'(x) &= \frac{1}{\mathrm{EI}_2} \left(M_{\mathrm{A}} x + R_{\mathrm{A}} \frac{x^2}{2} - P \frac{x^2}{2} + PLx + G_3 \right), \\ v_{II}(x) &= \frac{1}{\mathrm{EI}_2} \left(M_{\mathrm{A}} \frac{x^2}{2} + R_{\mathrm{A}} \frac{x^3}{6} - P \frac{x^3}{6} + PL \frac{x^2}{2} + G_3 x + G_4 \right). \end{aligned} \tag{47}$$

Using the above expressions (47) in Eqs. (44) and (45), one obtains 5 equations which together with the 2 equations (43) and the relation $\mathrm{I}_1 = 2\,\mathrm{I}_2 = 2\,\mathrm{I}$ serve to compute all the 7 unknowns of the problem in the form

$$\begin{aligned} &G_1 = G_2 = 0, \quad G_3 = -11L^2 P/24, \quad G_4 = 19L^3 P/108, \\ &M_{\mathrm{A}} = -4PL/9, \quad R_{\mathrm{A}} = 13P/18, \quad R_{\mathrm{C}} = 5P/18. \end{aligned} \tag{48}$$

Thus, one can finally determine

$$\begin{aligned} v_2 &= v_I\,(L) = -\frac{11}{216} \frac{PL^3}{\mathrm{EI}}, \\ v_3' &= v_{II}'\,(2L) = \frac{7}{72} \frac{PL^2}{\mathrm{EI}}, \\ V_1 &= R_{\mathrm{A}} = \frac{13}{18} P, \end{aligned} \tag{49}$$

which coincide with those of (40)–(42) when $g = 0$ through a limiting process.

Figure 13 depicts the normalized deflection v_2/v_2^{c}, where $v_2^{\mathrm{c}} = -11PL^3/216\mathrm{EI}$ is the classical one, versus g/L. From this figure, one can easily observe the decrease of the deflection v_2 for increasing values of the gradient coefficient g (stiffening effect in gradient elasticity).

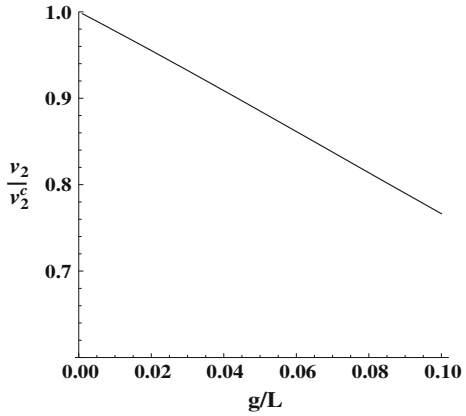

Fig. 13 Deflection versus distance for various values of g/L of the beam structure of Fig. 11

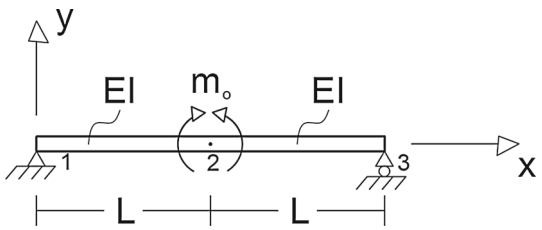

Fig. 14 Simply supported beam under a double moment at its mid-span

Example 4 Consider a simply supported beam of flexural rigidity EI and length $2L$ under the action of a double moment m_o at its midspan, as shown in Fig. 14. This example is similar to example 2 (same geometry and boundary conditions). The only difference has to do with the force vector $\{F\}$ which is now of the form

$$\{F\} = \{0, 0, m_o, 0\}^T . \tag{50}$$

The solution is obtained analytically with the aid of Mathematica [23] and has the form

$$\begin{aligned} v_1' &= -v_3' = (m_o/2\text{EI})\,[1 - \text{sech}\,(L/g)]\,, \\ v_2 &= (m_o/2\text{EI})\,[g\tanh\,(L/g) - L]\,, \\ v_2'' &= -\,(m_o/2g\text{EI})\,\tanh\,(L/g)\,. \end{aligned} \tag{51}$$

The reactions at nodes 1 and 3 take the form

$$\begin{aligned} V_1 &= V_3 = 0, \\ m_1 &= m_3 = -\,(m_o/2)\,\text{sech}\,(L/g)\,. \end{aligned} \tag{52}$$

It is observed that when the load is of a microstructural nature, the classical reactions are zero and there are only microstructural reactions and microstructural deformation.

Example 5 Consider a simply supported gradient elastic beam of flexural rigidity EI and length L subjected to a uniformly distributed load q, as shown in Fig. 15. The beam is considered to be one finite element 1–2 under the action of the equivalent nodal loads (24)—actually under $M(0)$, $M(L)$, $m(0)$ and $m(L)$, since $V(0)$ and $V(L)$ are absorbed by the vertical reactions. In the finite element convention of Fig. 3, these equivalent nodal loads have the form

$$\begin{aligned} M^f(0) &= M(0), \quad M^f(L) = -M(0), \\ m^f(0) &= m(0), \quad m^f(L) = m(0), \end{aligned} \tag{53}$$

where the superscript f denotes finite element convention.

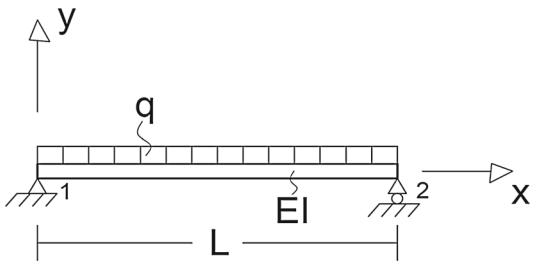

Fig. 15 Simply supported beam under a uniformly distributed load q

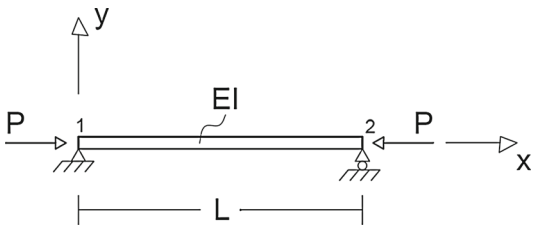

Fig. 16 Geometry of a simply supported gradient elastic beam under an axial compressive load

The boundary conditions of the problem read

$$v_1 = v_2 = 0 \tag{54}$$

and in the stiffness equation (8), the matrix $[K]$ is of the order 4×4, while the vectors $\{F\}$ and $\{U\}$ have the form

$$\begin{aligned} \{F\} &= \left\{M^f(0), m^f(0), M^{\mathrm{f}}(L), m^f(L)\right\}^{\mathrm{T}}, \\ \{U\} &= \left\{v_1', v_1'', v_2', v_2''\right\}^{\mathrm{T}}. \end{aligned} \tag{55}$$

Thus, one solves the 4×4 matrix equation (8) with the aid of Mathematica [23] and obtains the unknown vector $\{U\}$ of Eq. (55) as

$$\begin{aligned} v_1' &= -v_2' = \frac{L^2 q \operatorname{csch}\left[\frac{L}{4g}\right]\left(2gL - 5gL\cosh\left[\frac{L}{2g}\right] + (6g^2 + L^2)\sinh\left[\frac{L}{2g}\right]\right)}{48\mathrm{EI}\left(L\cosh\left[\frac{L}{4g}\right] - 4g\sinh\left[\frac{L}{4g}\right]\right)}, \\ v_1'' &= v_2'' \\ &= \frac{q\left(288g^2 L\cosh\left[\frac{L}{4g}\right] + 3L^2\left(-12g + L\coth\left[\frac{L}{4g}\right]\right)\operatorname{csch}\left[\frac{L}{4g}\right] - L\left(96g^2 + L^2\right)\operatorname{sech}\left[\frac{L}{4g}\right] - 48g\left(8g^2 + L^2\right)\sinh\left[\frac{L}{4g}\right]\right)}{96\mathrm{EI}\left(L\cosh\left[\frac{L}{4g}\right] - 4g\sinh\left[\frac{L}{4g}\right]\right)}. \end{aligned} \tag{56}$$

Example 6 Consider a simply supported gradient elastic uniform beam under the action of an axial compressive force P, as shown in Fig. 16. The beam has length L and flexural rigidity EI. Use will be made of the FEM to determine the critical or buckling load P_{cr}.

The beam of Fig. 16 is considered to be one finite element with nodes 1 and 2 and 3 d.o.f. per node. Thus, the structural stiffness matrix $[S]$ of this beam is of order 6×6 and connects generalized nodal forces to nodal displacements by Eq. (27). The classical boundary conditions in terms of displacements are

$$v_1 = v_2 = 0, \tag{57}$$

while the nonclassical ones in terms of generalized displacements are assumed to be

$$v_1'' = v_2'' = 0. \tag{58}$$

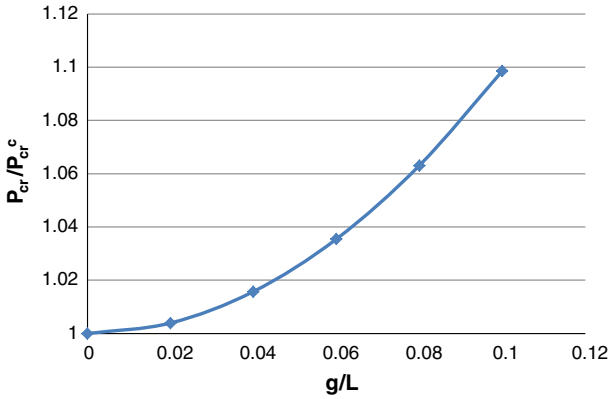

Fig. 17 Variation of the dimensionless buckling load $P_{\rm cr}/P_{\rm cr}^{\rm c}$ versus g/L for the beam of Fig. 16 under B.C. (57) and (58)

Application of the above 4 boundary conditions reduces Eq. (27) to

$$\begin{Bmatrix} M_1 \\ M_2 \end{Bmatrix} = \begin{bmatrix} S_{22} & S_{25} \\ S_{52} & S_{55} \end{bmatrix} \begin{Bmatrix} v_1' \\ v_2' \end{Bmatrix}, \tag{59}$$

where the stability stiffness coefficients S_{22}, $S_{25} = S_{52}$, S_{55} are given in Appendix 2.

The critical load $P_{\rm cr}$ is found by solving the determinant equation

$$S_{22}S_{55} - S_{25}^2 = 0 \tag{60}$$

for P and keeping the first root of the solution. Indeed, substitution in (60) of the coefficients S_{22}, S_{55} and S_{25} with their expressions in Appendix 2 yields

$$P_{\rm cr} = \frac{\pi^2 {\rm EI}}{L^2}\left[1 + \pi^2\left(\frac{g}{L}\right)^2\right] \tag{61}$$

which is exactly the same with that found in [11] analytically. Figure 17 depicts the variation of $\mathrm{P_{cr}/P_{cr}^{c}}$ versus g/L, where $\mathrm{P_{cr}^{c}} = \pi^2 \mathrm{EI}/L^2$ is the classical value of $\mathrm{P_{cr}}$, and clearly shows an increase of this dimensionless buckling ratio for increasing values of the dimensionless gradient coefficient g/L with a constantly increasing rate of increase.

Example 7 Consider the beam of the previous example with the same geometrical and physical properties and the same loading. The problem is here to determine the $\mathrm{P_{cr}}$ under the same classical boundary conditions (57) but different nonclassical boundary conditions than those of Eq. (58). The nonclassical boundary conditions are assumed here to be

$$m_1 = m_2 = 0 \tag{62}$$

or equivalently, in view of $(10)_3$,

$$v'''(0) = v'''(L) = 0. \tag{63}$$

Use of the classical boundary conditions (57) in the stiffness equation (27) reduces it to the explicit form

$$\begin{aligned} M_1 &= S_{22}v_1' + S_{23}v_1'' + S_{25}v_2' + S_{26}v_2'', \\ m_1 &= S_{32}v_1' + S_{33}v_1'' + S_{35}v_2' + S_{36}v_2'', \\ M_2 &= S_{52}v_1' + S_{53}v_1'' + S_{55}v_2' + S_{56}v_2'', \\ m_2 &= S_{62}v_1' + S_{63}v_1'' + S_{65}v_2' + S_{66}v_2''. \end{aligned} \tag{64}$$

In finite element analysis, boundary conditions are in terms of generalized nodal displacements. Unfortunately, nonclassical conditions (63), which are in terms of generalized displacements, do not correspond to element degrees of freedom even though they satisfy the variational boundary conditions $(6)_3$ and hence are legitimate boundary conditions. In this problem, the only way to impose those conditions in the finite element setting of

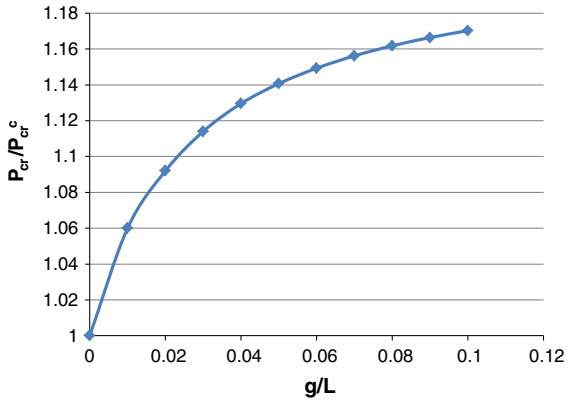

Fig. 18 Variation of the dimensionless buckling load $P_{\rm cr}/P_{\rm cr}^{\rm c}$ versus g/L for the beam of Fig. 16 under B.C. (57) and (62) or (63)

Eq. (64) is by using them in the form of Eq. (62) and letting $m_1 = m_2 = 0$ in Eq. (64). Thus, by solving Eq. $(64)_2$ and $(64)_4$ with $m_1 = m_2 = 0$ for v_2' and v_2'' in terms of v_1' and v_1'', one can eliminate v_2' and v_2'' from Eq. $(64)_1$ and $(64)_3$ and obtain the matrix equation

$$\left\{ \begin{array}{c} M_1 \\ M_2 \end{array} \right\} = \left[\begin{array}{cc} S_\alpha & S_\gamma \\ S_\gamma & S_\beta \end{array} \right] \left\{ \begin{array}{c} v_1' \\ v_1'' \end{array} \right\}, \tag{65}$$

where S_α, S_β and S_γ are stiffness coefficients in the form of complicated algebraic expressions involving the coefficients S_{ij} in Eq. (64) and obtained with the aid of Mathematica [23].

In order to determine the critical load of the beam in this example, the determinant of the stiffness matrix in Eq. (65) is set equal to zero and the numerically obtained first root of the resulting equation is the critical load $\rm P_{cr}$. Figure 18 shows the $\rm P_{cr}/P_{cr}^{c}$ dimensionless buckling ratio versus the dimensionless gradient coefficient g/L and exhibits an increase of this buckling ratio for increasing values of the gradient ratio as in Fig. 18. However, the rate of increase here constantly decreases in contrast to the previous case of Fig. 17 with different nonclassical boundary conditions. This is in agreement with recent results in two-dimensional gradient elasticity [24] indicating the significant effect of nonclassical boundary conditions on the structural response to static loading.

For verification reasons, the same problem was also solved analytically by imposing the boundary conditions (57), (63) and

$$M(0) = M(L) = 0 \tag{66}$$

implying due to Eq. $(10)_2$

$$v''(0) - g^2 v^{\rm IV}(0) = v''(L) - g^2 v^{\rm IV}(L) = 0. \tag{67}$$

For the implementation of these 6 boundary conditions, one needs to compute from $v(x)$ of Eq. (25) the derivatives

$$\begin{aligned} v''(x) &= -\xi^2 C_3 \sin\xi x - \xi^2 C_4 \cos\xi x + \theta^2 C_5 \sinh\theta x + \theta^2 C_6 \cosh\theta x, \\ v'''(x) &= -\xi^3 C_3 \cos\xi x + \xi^3 C_4 \sin\xi x + \theta^3 C_5 \cosh\theta x + \theta^3 C_6 \sinh\theta x, \\ v^{\rm IV}(x) &= -\xi^4 C_3 \sin\xi x + \xi^4 C_4 \cos\xi x + \theta^4 C_5 \sinh\theta x + \theta^4 C_6 \cosh\theta x. \end{aligned} \tag{68}$$

Imposing conditions (57), (63) and (67) on Eqs. (25) and (68) results in a system of 6 linear equations with 6 unknowns $(C_1, C_2, \ldots, C_6)$ reading as

$$\begin{aligned} &C_2 + C_4 + C_6 = 0, \\ &-\xi^3 C_3 + \theta^3 C_5 = 0, \\ &LC_1 + C_2 + (\sin\xi L) C_3 + (\cos\xi L) C_4 + (\sinh\theta L) C_5 + (\cosh\theta L) C_6 = 0, \\ &(-\xi^3 \cos\xi L) C_3 + (\xi^3 \sin\xi L) C_4 + (\theta^3 \cosh\theta L) C_5 + (\theta^3 \sinh\theta L) C_6 = 0, \\ &-\xi^2 (1 + g^2 \xi^2) C_4 + \theta^2 (1 - g^2 \theta^2) C_6 = 0, \end{aligned}$$

$$-\xi^2(1+g^2\xi^2)(\sin\xi L)C_3+\xi^2(1+g^2\xi^2)(\cos\xi L)C_4+\theta^2(1-g^2\theta^2)(\sinh\theta L)C_5$$
$$+\theta^2(1-g^2\theta^2)(\cosh\theta L)C_6=0. \tag{69}$$

For the above homogeneous system of linear equations to have non zero solutions, the determinant of the coefficients of the unknowns $C_1, C_2, \ldots, C_6$ is set equal to zero. Thus, one can numerically obtain the first root of the resulting equation, which is the critical load P_{cr}. The results of this method were found to be exactly the same as those obtained by the FEM and depicted in Fig. 18.

7 Conclusions

On the basis of the results presented in the previous sections, the following conclusions can be stated:

1. A finite element for a gradient elastic Bernoulli–Euler beam in bending under static loading has been developed with two nodes (at the ends of the element) and three degrees of freedom per node, the displacement, the slope and the curvature.
2. The displacement function of this formulation was selected to be the exact solution of the governing equation of equilibrium of the beam resulting in the exact element stiffness matrix with all its entries expressed in closed form. As a result, use of this matrix in a finite element analysis provides the exact response of a beam structure to static loading.
3. When the effect of an axial compressive load on bending is taken into account in the development of the stiffness matrix of the flexural beam element and use is made of the exact solution of the buckling governing equation as the displacement function, the exact stability stiffness matrix of an element is obtained. This leads to the exact value of the critical or buckling load.
4. Seven examples are presented in detail to illustrate the method and demonstrate its advantages when applied to problems of static and stability analysis of plane gradient elastic beam structures. In almost all cases, the results are verified by analytic solutions obtained here or taken from the literature.
5. The advantages of the FEM presented here are generality, versatility, easy and systematic way of treatment, computational efficiency and obtaining of the exact structural response or buckling load.
6. It was observed, at least in all the examples considered here, a decrease of deflections and an increase of the buckling loads for increasing values of the gradient coefficient, in agreement with the well-known stiffening effect in gradient elasticity. It was also observed, at least in the buckling examples considered here, the significant effect of the nonclassical boundary conditions on the response, which dictate the rate of increase of the buckling loads for increasing values of the gradient coefficient.

Appendix 1

Explicit expressions for the stiffness coefficients K_{ij} of the stiffness matrix [K] for a gradient elastic flexural beam element:

$$K_{11}=\frac{12\mathrm{EI}}{12g^2L+L^3-6gL^2\coth\left[\frac{L}{2g}\right]}$$

$$K_{21}=-\frac{6\mathrm{EI}}{12g^2+L^2-6gL\coth\left[\frac{L}{2g}\right]}$$

$$K_{22}=-\frac{4\mathrm{EI}\left(-3gL\cosh\left[\frac{L}{g}\right]+(3g^2+L^2)\sinh\left[\frac{L}{g}\right]\right)}{24g^3-4gL^2-8g(3g^2+L^2)\cosh\left[\frac{L}{g}\right]+L(24g^2+L^2)\sinh\left[\frac{L}{g}\right]}$$

$$K_{31}=\mathrm{EI}\left(\frac{1}{L}-\frac{L}{12g^2+L^2-6gL\coth\left[\frac{L}{2g}\right]}\right)$$

$$K_{32}=-\frac{2\mathrm{EI}g\left(-12g^2+L^2+2(6g^2+L^2)\cosh\left[\frac{L}{g}\right]-9gL\sinh\left[\frac{L}{g}\right]\right)}{24g^3-4gL^2-8g(3g^2+L^2)\cosh\left[\frac{L}{g}\right]+L(24g^2+L^2)\sinh\left[\frac{L}{g}\right]}$$

$$K_{33} = \frac{\mathrm{EI}g\left((24g^4 - L^4)\cosh\left[\frac{L}{g}\right] + 4g\left(-6g^3 + 3gL^2 + (-6g^2L + L^3)\sinh\left[\frac{L}{g}\right]\right)\right)}{L(24g^3 - 4gL^2 - 8g(3g^2 + L^2)\cosh\left[\frac{L}{g}\right] + L\left(24g^2 + L^2\right)\sinh\left[\frac{L}{g}\right])}$$

$$K_{41} = -\frac{12\mathrm{EI}}{12g^2L + L^3 - 6gL^2\coth\left[\frac{L}{2g}\right]}$$

$$K_{42} = -\frac{6\mathrm{EI}}{12g^2 + L^2 - 6gL\coth\left[\frac{L}{2g}\right]}$$

$$K_{43} = \mathrm{EI}\left(\frac{1}{L} - \frac{L}{12g^2 + L^2 - 6gL\coth\left[\frac{L}{2g}\right]}\right)$$

$$K_{44} = \frac{12\mathrm{EI}}{12g^2L + L^3 - 6gL^2\coth\left[\frac{L}{2g}\right]}$$

$$K_{51} = -\frac{6\mathrm{EI}}{12g^2 + L^2 - 6gL\coth\left[\frac{L}{2g}\right]}$$

$$K_{52} = \frac{2\mathrm{EI}\left(6gL + (-6g^2 + L^2)\sinh\left[\frac{L}{g}\right]\right)}{4g(-6g^2 + L^2) + 8g(3g^2 + L^2)\cosh\left[\frac{L}{g}\right] - L(24g^2 + L^2)\sinh\left[\frac{L}{g}\right]}$$

$$K_{53} = \frac{2\mathrm{EI}gL\left(L\left(2 + \cosh\left[\frac{L}{g}\right]\right) - 3g\sinh\left[\frac{L}{g}\right]\right)}{4g(-6g^2 + L^2) + 8g(3g^2 + L^2)\cosh\left[\frac{L}{g}\right] - L(24g^2 + L^2)\sinh\left[\frac{L}{g}\right]}$$

$$K_{54} = \frac{6\mathrm{EI}}{12g^2 + L^2 - 6gL\coth\left[\frac{L}{2g}\right]}$$

$$K_{55} = -\frac{4\mathrm{EI}\left(-3gL\cosh\left[\frac{L}{g}\right] + (3g^2 + L^2)\sinh\left[\frac{L}{g}\right]\right)}{24g^3 - 4gL^2 - 8g(3g^2 + L^2)\cosh\left[\frac{L}{g}\right] + L(24g^2 + L^2)\sinh\left[\frac{L}{g}\right]}$$

$$K_{61} = \mathrm{EI}\left(-\frac{1}{L} + \frac{L}{12g^2 + L^2 - 6gL\coth\left[\frac{L}{2g}\right]}\right)$$

$$K_{62} = \frac{2\mathrm{E}g\mathrm{I}L\left(L\left(2 + \cosh\left[\frac{L}{g}\right]\right) - 3g\sinh\left[\frac{L}{g}\right]\right)}{24g^3 - 4gL^2 - 8g(3g^2 + L^2)\cosh\left[\frac{L}{g}\right] + L(24g^2 + L^2)\sinh\left[\frac{L}{g}\right]}$$

$$K_{63} = \frac{\mathrm{E}g\mathrm{I}\left(24g^4 + L^4 + 2g\left(-6g(2g^2 + L^2)\cosh\left[\frac{L}{g}\right] + L(12g^2 + L^2)\sinh\left[\frac{L}{g}\right]\right)\right)}{L\left(24g^3 - 4gL^2 - 8g(3g^2 + L^2)\cosh\left[\frac{L}{g}\right] + L(24g^2 + L^2)\sinh\left[\frac{L}{g}\right]\right)}$$

$$K_{64} = \mathrm{EI}\left(\frac{1}{L} - \frac{L}{12g^2 + L^2 - 6gL\coth\left[\frac{L}{2g}\right]}\right)$$

$$K_{65} = \frac{2\mathrm{E}g\mathrm{I}\left(-12g^2 + L^2 + 2(6g^2 + L^2)\cosh\left[\frac{L}{g}\right] - 9gL\sinh\left[\frac{L}{g}\right]\right)}{24g^3 - 4gL^2 - 8g(3g^2 + L^2)\cosh\left[\frac{L}{g}\right] + L(24g^2 + L^2)\sinh\left[\frac{L}{g}\right]}$$

$$K_{66} = \frac{\mathrm{E}g\mathrm{I}\left((24g^4 - L^4)\cosh\left[\frac{L}{g}\right] + 4g\left(-6g^3 + 3gL^2 + (-6g^2L + L^3)\sinh\left[\frac{L}{g}\right]\right)\right)}{L\left(24g^3 - 4gL^2 - 8g(3g^2 + L^2)\cosh\left[\frac{L}{g}\right] + L(24g^2 + L^2)\sinh\left[\frac{L}{g}\right]\right)}$$

Appendix 2

Explicit expressions for the stiffness coefficients S_{ij} of the stability stiffness matrix [S] for a gradient elastic flexural beam element with a compressive axial force:

$$S_{11} = -\frac{\theta^2\xi^2\left(\theta(-1+c\theta^2)\cosh\left[\frac{\theta}{2}\right]\sin\left[\frac{\xi}{2}\right]+\xi(1+c\xi^2)\cos\left[\frac{\xi}{2}\right]\sinh\left[\frac{\theta}{2}\right]\right)}{\theta\xi^2\cosh\left[\frac{\theta}{2}\right]\sin\left[\frac{\xi}{2}\right]+\left(\theta^2\xi\cos\left[\frac{\xi}{2}\right]-2(\theta^2+\xi^2)\sin\left[\frac{\xi}{2}\right]\right)\sinh\left[\frac{\theta}{2}\right]}$$

$$\begin{aligned}
S_{21} = {} & -((c\theta^2\xi^2(\theta^2+\xi^2)(-\xi\sin[\xi]+\xi\cosh[\theta]\sin[\xi] \\
& +\theta(-1+\cos[\xi])\sinh[\theta])))/((-2\xi\cosh[\theta](\theta^2\xi\cos[\xi] \\
& -(\theta^2+\xi^2)\sin[\xi])-2\xi(-\theta^2\xi+(\theta^2+\xi^2)\sin[\xi]) \\
& +\theta(-2(\theta^2+\xi^2)+2(\theta^2+\xi^2)\cos[\xi]+\xi(\theta^2-\xi^2)\sin[\xi])\sinh[\theta]))
\end{aligned}$$

$$\begin{aligned}
S_{22} = {} & -((c\theta\xi(\theta^2+\xi^2)(\theta\xi^2\cosh[\theta]\sin[\xi]+(\theta^2\xi\cos[\xi] \\
& -(\theta^2+\xi^2)\sin[\xi])\sinh[\theta])))/((-2\xi\cosh[\theta](\theta^2\xi\cos[\xi] \\
& -(\theta^2+\xi^2)\sin[\xi])-2\xi(-\theta^2\xi+(\theta^2+\xi^2)\sin[\xi])+\theta(-2(\theta^2+\xi^2)+2(\theta^2 \\
& +\xi^2)\cos[\xi]+\xi(\theta^2-\xi^2)\sin[\xi])\sinh[\theta]))
\end{aligned}$$

$$\begin{aligned}
S_{31} = {} & ((c\theta^2\xi^2(\theta^2-\xi^2-\theta^2\cos[\xi]-\xi^2\cos[\xi]+(\theta^2+\xi^2+(-\theta^2+\xi^2)\cos[\xi])\cosh[\theta] \\
& -2\theta\xi\sin[\xi]\sinh[\theta])))/((-2\xi\cosh[\theta](\theta^2\xi\cos[\xi]-(\theta^2+\xi^2)\sin[\xi])-2\xi(-\theta^2\xi+(\theta^2+\xi^2)\sin[\xi]) \\
& +\theta(-2(\theta^2+\xi^2)+2(\theta^2+\xi^2)\cos[\xi]+\xi(\theta^2-\xi^2)\sin[\xi])\sinh[\theta]))
\end{aligned}$$

$$\begin{aligned}
S_{32} = {} & ((c\theta\xi(-\theta(-\theta^2\xi+\xi^3+(\theta^2+\xi^2)\sin[\xi])+\cosh[\theta]((-\theta^3\xi+\theta\xi^3)\cos[\xi]+\theta(\theta^2+\xi^2)\sin[\xi]) \\
& +\xi(\theta^2+\xi^2-(\theta^2+\xi^2)\cos[\xi]-2\theta^2\xi\sin[\xi])\sinh[\theta])))/((-2\xi\cosh[\theta](\theta^2\xi\cos[\xi] \\
& -(\theta^2+\xi^2)\sin[\xi])-2\xi(-\theta^2\xi+(\theta^2+\xi^2)\sin[\xi])+\theta(-2(\theta^2+\xi^2)+2(\theta^2+\xi^2)\cos[\xi] \\
& +\xi(\theta^2-\xi^2)\sin[\xi])\sinh[\theta]))
\end{aligned}$$

$$\begin{aligned}
S_{33} = {} & ((c(-\cosh[\theta](2(\theta^4+\theta^2\xi^2+\xi^4)\cos[\xi]+\theta^2(\theta^2+\xi^2)(-2+\xi\sin[\xi])) \\
& +\xi(2\xi(-\theta^2+(\theta^2+\xi^2)\cos[\xi])+\theta(\xi(\theta^2+\xi^2)\cos[\xi] \\
& +(-\theta^2+\xi^2)\sin[\xi])\sinh[\theta])))/((-2\xi\cosh[\theta](\theta^2\xi\cos[\xi]-(\theta^2+\xi^2)\sin[\xi]) \\
& -2\xi(-\theta^2\xi+(\theta^2+\xi^2)\sin[\xi])+\theta(-2(\theta^2+\xi^2)+2(\theta^2+\xi^2)\cos[\xi]+\xi(\theta^2-\xi^2)\sin[\xi])\sinh[\theta]))
\end{aligned}$$

$$S_{41} = \frac{\theta^2\xi^2(\theta(-1+c\theta^2)\cosh\left[\frac{\theta}{2}\right]\sin\left[\frac{\xi}{2}\right]+\xi(1+c\xi^2)\cos\left[\frac{\xi}{2}\right]\sinh\left[\frac{\theta}{2}\right])}{\theta\xi^2\cosh\left[\frac{\theta}{2}\right]\sin\left[\frac{\xi}{2}\right]+(\theta^2\xi\cos\left[\frac{\xi}{2}\right]-2(\theta^2+\xi^2)\sin\left[\frac{\xi}{2}\right])\sinh\left[\frac{\theta}{2}\right]}$$

$$\begin{aligned}
S_{42} = {} & -((\theta\xi(\theta^2+\xi^2)(\theta(-\xi(1-c\theta^2+c\xi^2)\cos[\xi] \\
& +\sin[\xi]-c\theta^2\sin[\xi])+\theta\cosh[\theta](\xi-c\theta^2\xi+c\xi^3+(-1+c\theta^2)\sin[\xi]) \\
& -2\xi\left(1+c\xi^2\right)\sin\left[\frac{\xi}{2}\right]^2\sinh[\theta])))/((-2\xi\cosh[\theta](\theta^2\xi\cos[\xi]-(\theta^2+\xi^2)\sin[\xi]) \\
& -2\xi(-\theta^2\xi+(\theta^2+\xi^2)\sin[\xi])+\theta(-2(\theta^2+\xi^2)+2(\theta^2+\xi^2)\cos[\xi]+\xi(\theta^2-\xi^2)\sin[\xi])\sinh[\theta]))
\end{aligned}$$

$$\begin{aligned}
S_{43} = {} & ((-2\theta^4+2c\theta^6-2\theta^2\xi^2+c\theta^4\xi^2-2\xi^4 \\
& -c\theta^2\xi^4-2c\xi^6+2\theta^4\cos[\xi]-2c\theta^6\cos[\xi]+2\theta^2\xi^2\cos[\xi]-c\theta^4\xi^2\cos[\xi]+c\theta^2\xi^4\cos[\xi] \\
& +\xi^2(-(\theta^2+\xi^2)(-2+c\theta^2-2c\xi^2)+\theta^2(-2+c\theta^2-c\xi^2)\cos[\xi])\cosh[\theta]+\theta^4\xi\sin[\xi] \\
& -c\theta^6\xi\sin[\xi] \\
& +\theta^2\xi^3\sin[\xi]+c\theta^2\xi^5\sin[\xi]-\theta\xi(\xi(\theta^2-c\theta^4+\xi^2+c\xi^4)+(-\theta^2+c\theta^4 \\
& +\xi^2+c\xi^4)\sin[\xi])\sinh[\theta]))/((-2\xi\cosh[\theta](\theta^2\xi\cos[\xi]-(\theta^2+\xi^2)\sin[\xi]) \\
& -2\xi(-\theta^2\xi+(\theta^2+\xi^2)\sin[\xi])+\theta(-2(\theta^2+\xi^2)+2(\theta^2+\xi^2)\cos[\xi]+\xi(\theta^2-\xi^2)\sin[\xi])\sinh[\theta]))
\end{aligned}$$

$$S_{44} = -\frac{\theta^2\xi^2(\theta(-1+c\theta^2)\cosh\left[\frac{\theta}{2}\right]\sin\left[\frac{\xi}{2}\right]+\xi(1+c\xi^2)\cos\left[\frac{\xi}{2}\right]\sinh\left[\frac{\theta}{2}\right])}{\theta\xi^2\cosh\left[\frac{\theta}{2}\right]\sin\left[\frac{\xi}{2}\right]+(\theta^2\xi\cos\left[\frac{\xi}{2}\right]-2(\theta^2+\xi^2)\sin\left[\frac{\xi}{2}\right])\sinh\left[\frac{\theta}{2}\right]}$$

$$
\begin{aligned}
S_{51} = &-((c\theta^2\xi^2(\theta^2+\xi^2)(-\xi\sin[\xi]+\xi\cosh[\theta]\sin[\xi]\\
&+\theta(-1+\cos[\xi])\sinh[\theta])))/((-2\xi\cosh[\theta](\theta^2\xi\cos[\xi]\\
&-\left(\theta^2+\xi^2\right)\sin[\xi])-2\xi(-\theta^2\xi+(\theta^2+\xi^2)\sin[\xi])+\theta(-2(\theta^2+\xi^2)\\
&+2(\theta^2+\xi^2)\cos[\xi]+\xi(\theta^2-\xi^2)\sin[\xi])\sinh[\theta]))\\
S_{52} = &((c\theta\xi(\theta^2+\xi^2)(\theta\xi^2\sin[\xi]-(-\theta^2\xi+(\theta^2+\xi^2)\sin[\xi])\sinh[\theta])))/((-2\xi\cosh[\theta](\theta^2\xi\cos[\xi]\\
&-(\theta^2+\xi^2)\sin[\xi])-2\xi(-\theta^2\xi+(\theta^2+\xi^2)\sin[\xi])+\theta(-2(\theta^2+\xi^2)+2(\theta^2+\xi^2)\cos[\xi]\\
&+\xi(\theta^2-\xi^2)\sin[\xi])\sinh[\theta]))\\
S_{53} = &-((c\theta\xi(\theta^2+\xi^2)(\theta(\xi\cos[\xi]-\sin[\xi])+\theta\cosh[\theta](-\xi+\sin[\xi])\\
&+(\xi-\xi\cos[\xi])\sinh[\theta])))/((-2\xi\cosh[\theta](\theta^2\xi\cos[\xi]-(\theta^2+\xi^2)\sin[\xi])-2\xi(-\theta^2\xi\\
&+(\theta^2+\xi^2)\sin[\xi])+\theta(-2(\theta^2+\xi^2)+2(\theta^2+\xi^2)\cos[\xi]+\xi(\theta^2-\xi^2)\sin[\xi])\sinh[\theta]))\\
S_{54} = &((c\theta^2\xi^2(\theta^2+\xi^2)(-\xi\sin[\xi]+\xi\cosh[\theta]\sin[\xi]\\
&+\theta(-1+\cos[\xi])\sinh[\theta])))/((-2\xi\cosh[\theta](\theta^2\xi\cos[\xi]\\
&-(\theta^2+\xi^2)\sin[\xi])-2\xi(-\theta^2\xi+(\theta^2+\xi^2)\sin[\xi])+\theta(-2(\theta^2+\xi^2)\\
&+2(\theta^2+\xi^2)\cos[\xi]+\xi(\theta^2-\xi^2)\sin[\xi])\sinh[\theta]))\\
S_{55} = &-((c\theta\xi(\theta^2+\xi^2)(\theta\xi^2\cosh[\theta]\sin[\xi]+(\theta^2\xi\cos[\xi]\\
&-(\theta^2+\xi^2)\sin[\xi])\sinh[\theta])))/((-2\xi\cosh[\theta](\theta^2\xi\cos[\xi]\\
&-(\theta^2+\xi^2)\sin[\xi])-2\xi(-\theta^2\xi+(\theta^2+\xi^2)\sin[\xi])+\theta(-2(\theta^2+\xi^2)\\
&+2(\theta^2+\xi^2)\cos[\xi]+\xi(\theta^2-\xi^2)\sin[\xi])\sinh[\theta]))\\
S_{61} = &(c\theta^2\xi^2(-\theta^2+\xi^2+\theta^2\cos[\xi]+\xi^2\cos[\xi]+(-\theta^2-\xi^2+(\theta^2-\xi^2)\cos[\xi])\cosh[\theta]\\
&+2\theta\xi\sin[\xi]\sinh[\theta]))/(-2\xi\cosh[\theta](\theta^2\xi\cos[\xi]-(\theta^2+\xi^2)\sin[\xi])-2\xi(-\theta^2\xi+(\theta^2+\xi^2)\sin[\xi])\\
&+\theta(-2(\theta^2+\xi^2)+2(\theta^2+\xi^2)\cos[\xi]+\xi(\theta^2-\xi^2)\sin[\xi])\sinh[\theta])\\
S_{62} = &((c\theta\xi(\theta^2+\xi^2)(\theta(\xi\cos[\xi]-\sin[\xi])+\theta\cosh[\theta](-\xi+\sin[\xi])\\
&+(\xi-\xi\cos[\xi])\sinh[\theta])))/((-2\xi\cosh[\theta](\theta^2\xi\cos[\xi]-(\theta^2+\xi^2)\sin[\xi])\\
&-2\xi(-\theta^2\xi+(\theta^2+\xi^2)\sin[\xi])\\
&+\theta(-2(\theta^2+\xi^2)+2(\theta^2+\xi^2)\cos[\xi]+\xi(\theta^2-\xi^2)\sin[\xi])\sinh[\theta]))\\
S_{63} = &(c(-2\theta^4-2\theta^2\xi^2-2\xi^4+2\theta^4\cos[\xi]+2\theta^2\xi^2\cos[\xi]+2\xi^2(\theta^2+\xi^2-\theta^2\cos[\xi])\cosh[\theta]\\
&+\theta^4\xi\sin[\xi]+\theta^2\xi^3\sin[\xi]-\theta\xi(\theta^2\xi+\xi^3\\
&-\theta^2\sin[\xi]+\xi^2\sin[\xi])\sinh[\theta]))/((-2\xi\cosh[\theta](\theta^2\xi\cos[\xi]-(\theta^2+\xi^2)\sin[\xi])\\
&-2\xi(-\theta^2\xi+(\theta^2+\xi^2)\sin[\xi])+\theta(-2(\theta^2+\xi^2)+2(\theta^2+\xi^2)\cos[\xi]+\xi(\theta^2-\xi^2)\sin[\xi])\sinh[\theta]))\\
S_{64} = &((c\theta^2\xi^2(\theta^2-\xi^2-\theta^2\cos[\xi]-\xi^2\cos[\xi]+(\theta^2+\xi^2+(-\theta^2+\xi^2)\cos[\xi])\cosh[\theta]\\
&-2\theta\xi\sin[\xi]\sinh[\theta]))/((-2\xi\cosh[\theta](\theta^2\xi\cos[\xi]-(\theta^2+\xi^2)\sin[\xi])-2\xi(-\theta^2\xi\\
&+(\theta^2+\xi^2)\sin[\xi])+\theta(-2(\theta^2+\xi^2)+2(\theta^2+\xi^2)\cos[\xi]+\xi(\theta^2-\xi^2)\sin[\xi])\sinh[\theta]))\\
S_{65} = &((c\theta\xi(\theta\cosh[\theta](\xi(\theta^2-\xi^2)\cos[\xi]-(\theta^2\\
&+\xi^2)\sin[\xi])+\theta(-\theta^2\xi+\xi^3+(\theta^2+\xi^2)\sin[\xi])+\xi(-\theta^2-\xi^2+(\theta^2+\xi^2)\cos[\xi]\\
&+2\theta^2\xi\sin[\xi])\sinh[\theta])))/((-2\xi\cosh[\theta](\theta^2\xi\cos[\xi]-(\theta^2+\xi^2)\sin[\xi])-2\xi(-\theta^2\xi\\
&+(\theta^2+\xi^2)\sin[\xi])+\theta(-2(\theta^2+\xi^2)+2(\theta^2+\xi^2)\cos[\xi]+\xi(\theta^2-\xi^2)\sin[\xi])\sinh[\theta]))\\
S_{66} = &((c(\theta^4\xi^2+\theta^2\xi^4-\theta^4\xi^2\cos[\xi]-\theta^2\xi^4\cos[\xi]-\theta^4\xi\sin[\xi]\\
&-7\theta^2\xi^3\sin[\xi]+\theta^4\xi\cos[\xi]\sin[\xi]+7\theta^2\xi^3\cos[\xi]\sin[\xi]+6\xi^5\cos[\xi]\sin[\xi]\\
&+\xi\cosh[\theta]^2(-\theta^2\left(\xi\left(\theta^2+\xi^2\right)\cos[2\xi]+\left(3\theta^2+\xi^2\right)\sin[\xi]\right)\\
&+\cos[\xi]\left(\theta^2\xi\left(\theta^2+\xi^2\right)+\left(3\theta^4+\theta^2\xi^2+2\xi^4\right)\sin[\xi]\right)\\
&+\theta\xi^2\left(4\left(-3\theta^2+\xi^2+\left(\theta^2+3\xi^2\right)\cos[\xi]\right)\sin\left[\frac{\xi}{2}\right]^2+\xi\left(\theta^2+\xi^2\right)\sin[2\xi]\right)\sinh[\theta]\\
&+\xi\left(-\theta^2\left(\xi\left(\theta^2+\xi^2\right)\cos[2\xi]+\left(3\theta^2+\xi^2\right)\sin[\xi]\right)\right.
\end{aligned}
$$

$$
\begin{aligned}
&+\cos[\xi]\left(\theta^2\xi\left(\theta^2+\xi^2\right)+\left(3\theta^4+\theta^2\xi^2+2\xi^4\right)\sin[\xi]\right))\sinh[\theta]^2\\
&+\cosh[\theta](-2\xi\sin[\xi]\left(2\left(\theta^4+2\theta^2\xi^2+2\xi^4\right)\cos[\xi]\right.\\
&\left.+\theta^2\left(-2\left(\theta^2+2\xi^2\right)+\xi\left(\theta^2+\xi^2\right)\sin[\xi]\right)\right)\\
&+\theta(5\theta^4+7\theta^2\xi^2+\xi^4-4\left(2\theta^4+2\theta^2\xi^2+\xi^4\right)\cos[\xi]+\left(\theta^4+\theta^2\xi^2+3\xi^4\right)\cos[2\xi]\\
&-2\theta^4\xi\sin[\xi]-2\theta^2\xi^3\sin[\xi]+\theta^4\xi\sin[2\xi]-\xi^5\sin[2\xi]\big)\sinh\big[\theta\big]\big)\\
&+\theta^5\cos[\xi]^2\sinh[2\theta])))/((2(-\xi\sin[\xi]+\xi\cosh[\theta]\sin[\xi]+\theta(-1\\
&+\cos[\xi])\sinh[\theta])(2\xi(-\theta^2\xi+(\theta^2+\xi^2)\sin[\xi])-2\xi\cosh[\theta](-\theta^2\xi\cos[\xi]\\
&+(\theta^2+\xi^2)\sin[\xi])+\theta(2(\theta^2+\xi^2)-2(\theta^2+\xi^2)\cos[\xi]+(-\theta^2\xi+\xi^3)\sin[\xi])\sinh[\theta])))
\end{aligned}
$$

References

1. Senturia, S.D.: Microsystem Design. Kluwer Academic Publishers, Boston (2001)
2. Mindlin, R.D.: Microstructure in linear elasticity. Arch. Ration. Mech. Anal. **16**, 51–78 (1964)
3. Exadaktylos, G.E., Vardoulakis, I.: Microstructure in linear elasticity and scale effects: a reconsideration of basic rock mechanics and rock fracture mechanics. Tectonophysics **335**, 81–109 (2001)
4. Askes, H., Aifantis, E.C.: Gradient elasticity in statics and dynamics: an overview of formulations, length scale identification procedures, finite element implementations and new results. Int. J. Solids Struct. **48**, 1962–1990 (2011)
5. Tsinopoulos, S.V., Polyzos, D., Beskos, D.E.: Static and dynamic BEM analysis of strain gradient elastic solids and structures. Comput. Model. Eng. Sci. (CMES) **86**, 113–144 (2012)
6. Papargyri-Beskou, S., Beskos, D.E.: Static analysis of gradient elastic bars, beams, plates and shells. Open Mech. J. **4**, 65–73 (2010)
7. Vardoulakis, I., Exadaktylos, G., Kourkoulis, S.K.: Bending of marble with intrinsic length scales: a gradient theory with surface energy and size effects. J. Phys. IV **8**, 399–406 (1998)
8. Georgiadis, H.G., Anagnostou, D.S.: Problems of Flamant-Boussinesq and Kelvin type in dipolar gradient elasticity. J. Elast. **90**, 71–98 (2008)
9. Papargyri-Beskou, S., Beskos, D.E.: Static, stability and dynamic analysis of gradient elastic flexural Kirchhoff plates. Arch. Appl. Mech. **78**, 625–635 (2008)
10. Papargyri-Beskou, S., Polyzos, D., Beskos, D.E.: Wave dispersion in gradient elastic solids and structures: a unified treatment. Int. J. Solids Struct. **46**, 3751–3759 (2009)
11. Papargyri-Beskou, S., Tsepoura, K.G., Polyzos, D., Beskos, D.E.: Bending and stability analysis of gradient elastic beams. Int. J. Solids Struct. **40**, 385–400 (2003)
12. Papargyri-Beskou, S., Polyzos, D., Beskos, D.E.: Dynamic analysis of gradient elastic flexural beams. Struct. Eng. Mech. **15**, 705–716 (2003)
13. Lam, D.C.C., Yang, F., Chong, A.C.M., Wang, J., Tong, P.: Experiments and theory in strain gradient elasticity. J. Mech. Phys. Solids **51**, 1477–1508 (2003)
14. Giannakopoulos, A.E., Stamoulis, K.: Structural analysis of gradient elastic components. Int. J. Solids Struct. **44**, 3440–3451 (2007)
15. Kong, S., Zhou, S., Nie, Z., Wang, K.: Static and dynamic analysis of micro beams based on strain gradient elasticity theory. Int. J. Eng. Sci. **47**, 487–498 (2009)
16. Wang, B., Zhao, J., Zhou, S.: A microscale Timoshenko beam model based on strain gradient elasticity theory. Eur. J. Mech. A/Solids **29**, 591–599 (2010)
17. Akgoz, B., Civalek, O.: A size-dependent shear deformation beam model based on the strain gradient elasticity theory. Int. J. Eng. Sci. **70**, 1–14 (2013)
18. Triantafyllou, A., Giannakopoulos, A.E.: Structural analysis using a dipolar elastic Timoshenko beam. Eur. J. Mech. A/Solids **39**, 218–228 (2013)
19. Martin, H.C.: Introduction to Matrix Methods of Structural Analysis. McGraw-Hill, New York (1966)
20. Artan, R., Batra, R.C.: Free vibrations of a strain gradient beam by the method of initial values. Acta Mech. **223**, 2393–2409 (2012)
21. Artan, R., Toksoz, A.: Stability analysis of gradient elastic beams by the method of initial value. Arch. Appl. Mech. **83**, 1129–1144 (2013)
22. Asiminas, E.L., Koumousis, V.K.: A beam finite element based on gradient elasticity. In: Beskos, D.E., Stavroulakis, G.E. (eds.) Proceedings of 10th HSTAM International Congress on Mechanics. Technical University of Crete Press, 25–27 May 2013, Chania, Crete, Greece, paper no 123
23. Mathematica, Version 4.1, Wolfram Research Inc., Champaign, IL, USA (2004)
24. Papargyri-Beskou, S., Tsinopoulos, S.V.: Lame's strain potential method for plane gradient elasticity problems. Arch. Appl. Mech. (to appear)